New dark matter search channels at electron colliders

Zuowei Liu (Nanjing University)

International Workshop on New Opportunities for Particle Physics 2024

July 19-21, 2024, IHEP, Beijing

Outline

1. New dark matter channel @ Belle II

   [Jinhan Liang, ZL, Lan Yang, JHEP, arXiv:2212.04252]

2. Belle II probes of strongly-interacting dark matter

   [Jinhan Liang, ZL, Lan Yang, PRD, arXiv:2312.08970]

1 New dark matter channel @ Belle II

[Liang, ZL, Yang, JHEP, arXiv:2212.04252]

Previous dark matter detection channels at colliders

Most studies focus on mono-X channel with SM X produced at the primary vertex

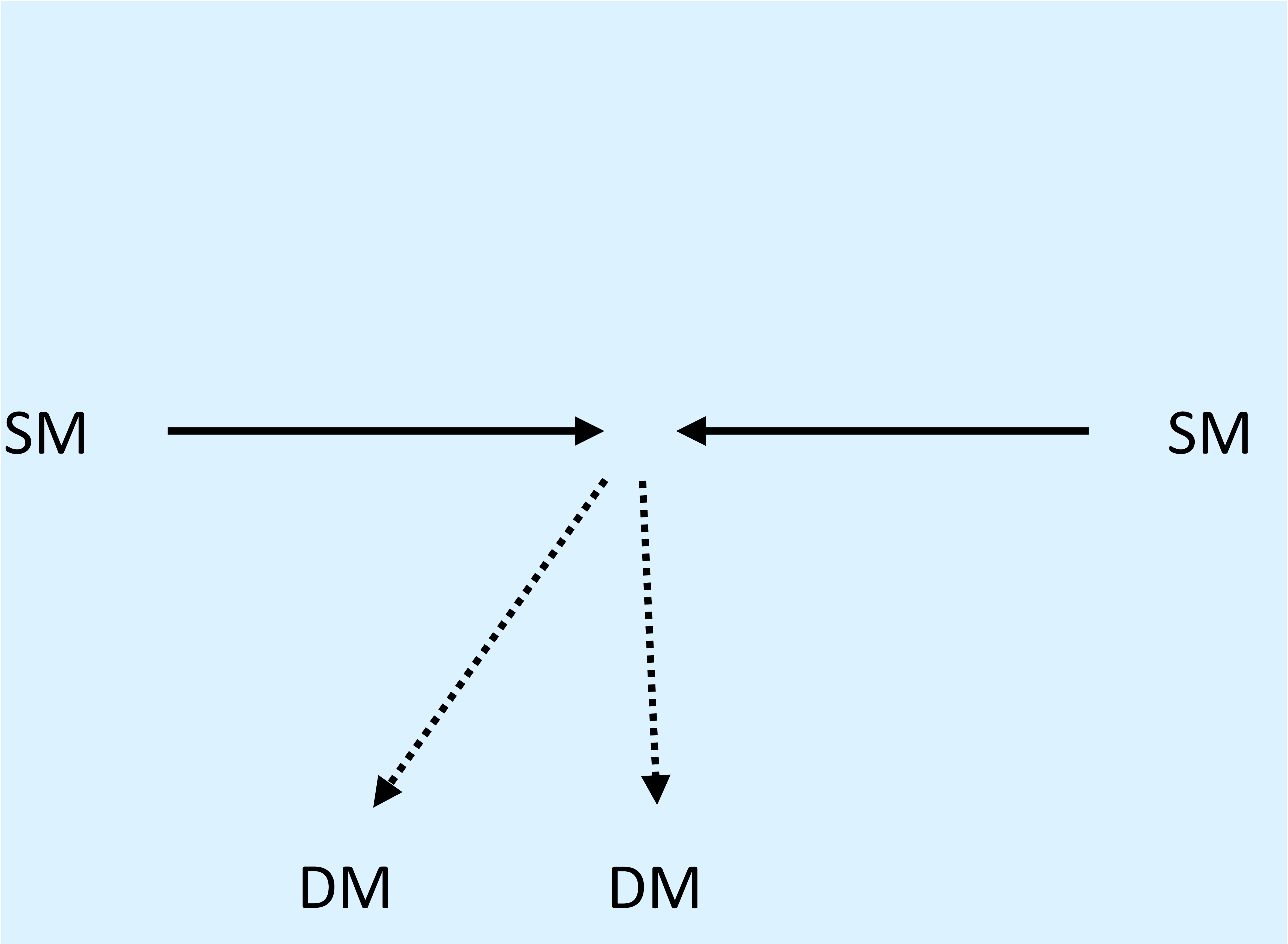

Previous dark matter detection channels at colliders

Most studies focus on mono-X channel with SM X produced at the primary vertex

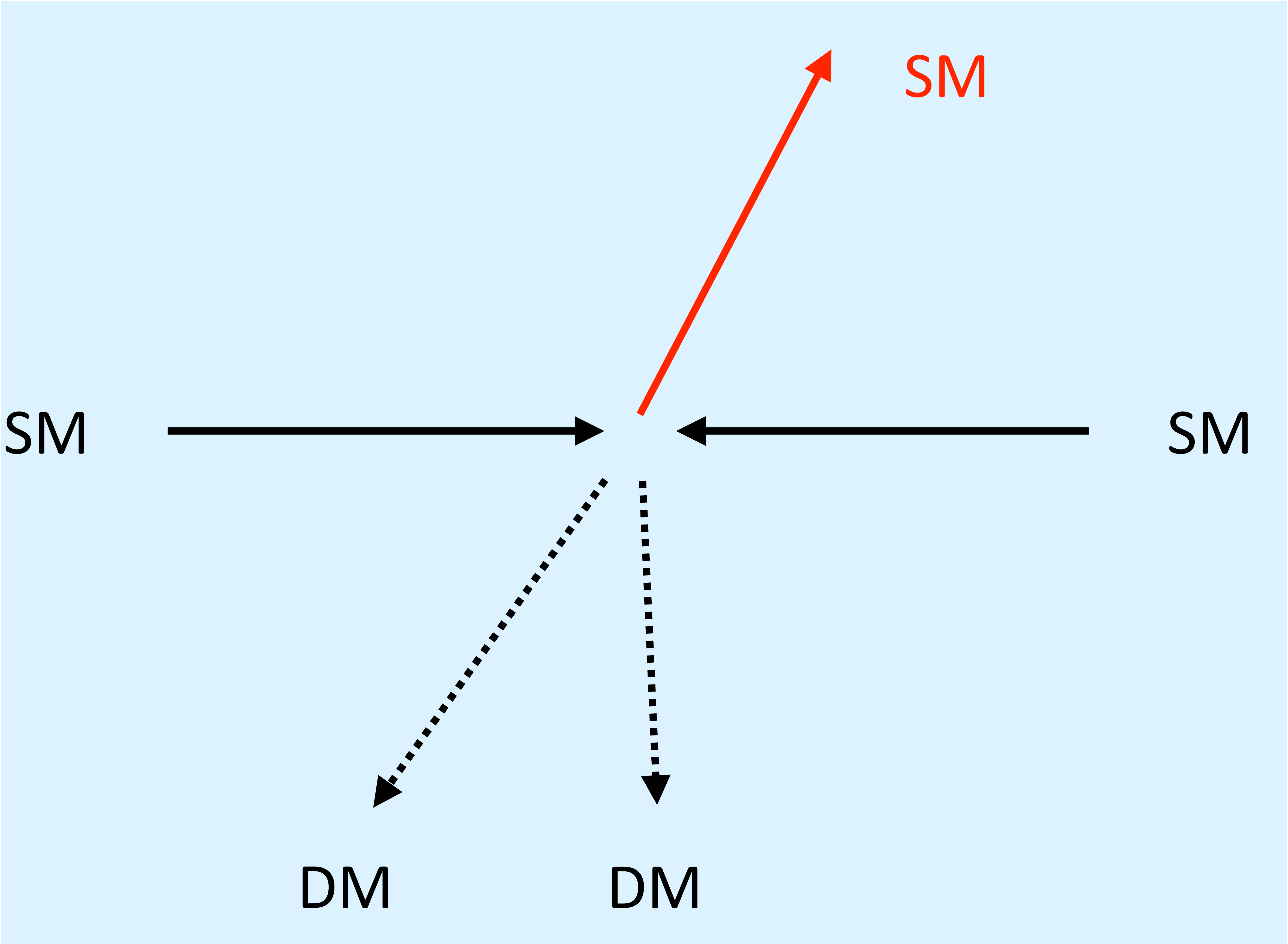

Previous dark matter detection channels at colliders

Most studies focus on mono-X channel with SM X produced at the primary vertex

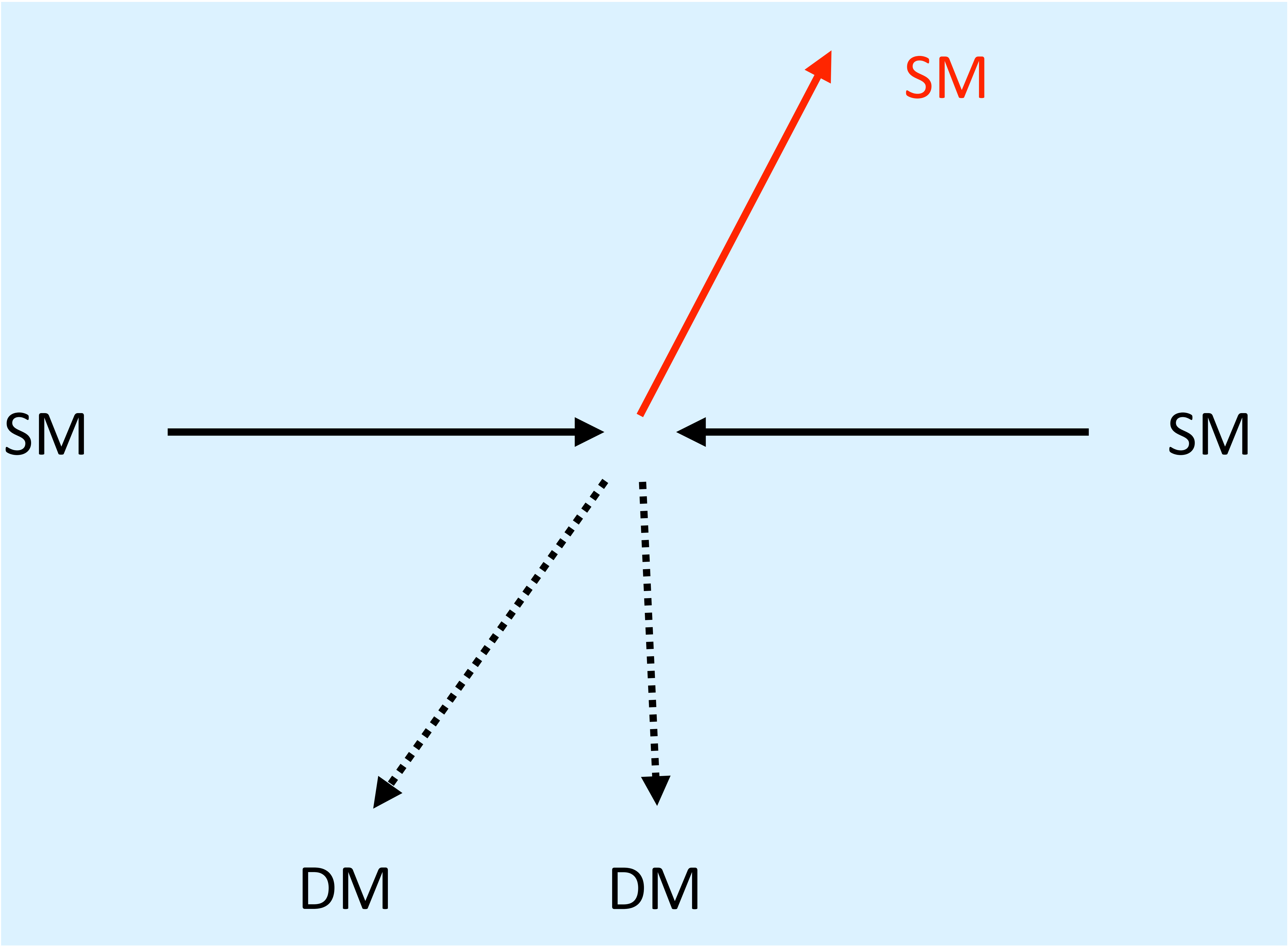

Different mono-X channels

- mono-photon
- mono-jet
- mono-Higgs
- mono-Z
- mono-top

We propose a new dark matter channel at colliders

We propose a new dark matter channel at colliders

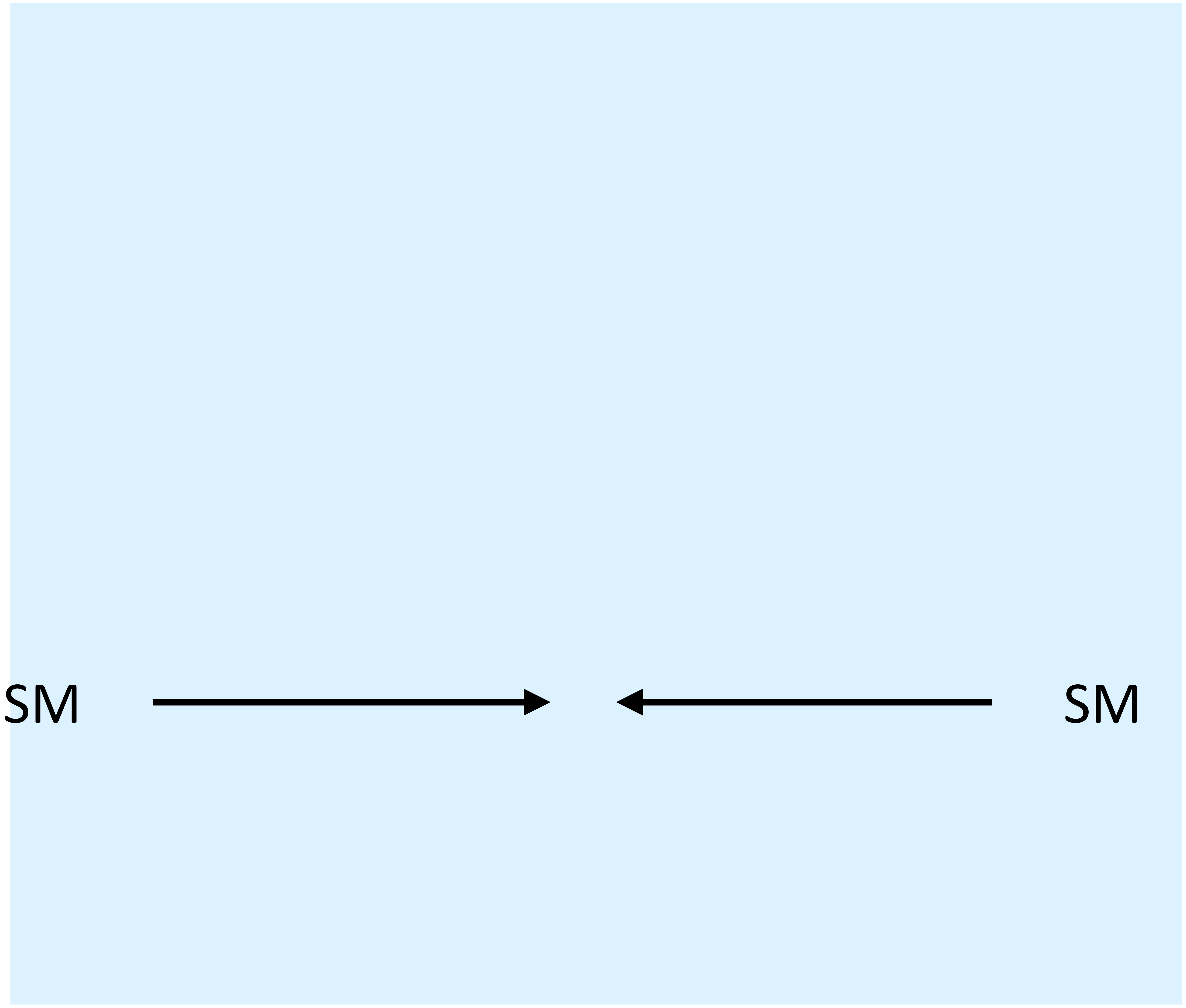

We propose a new dark matter channel at colliders

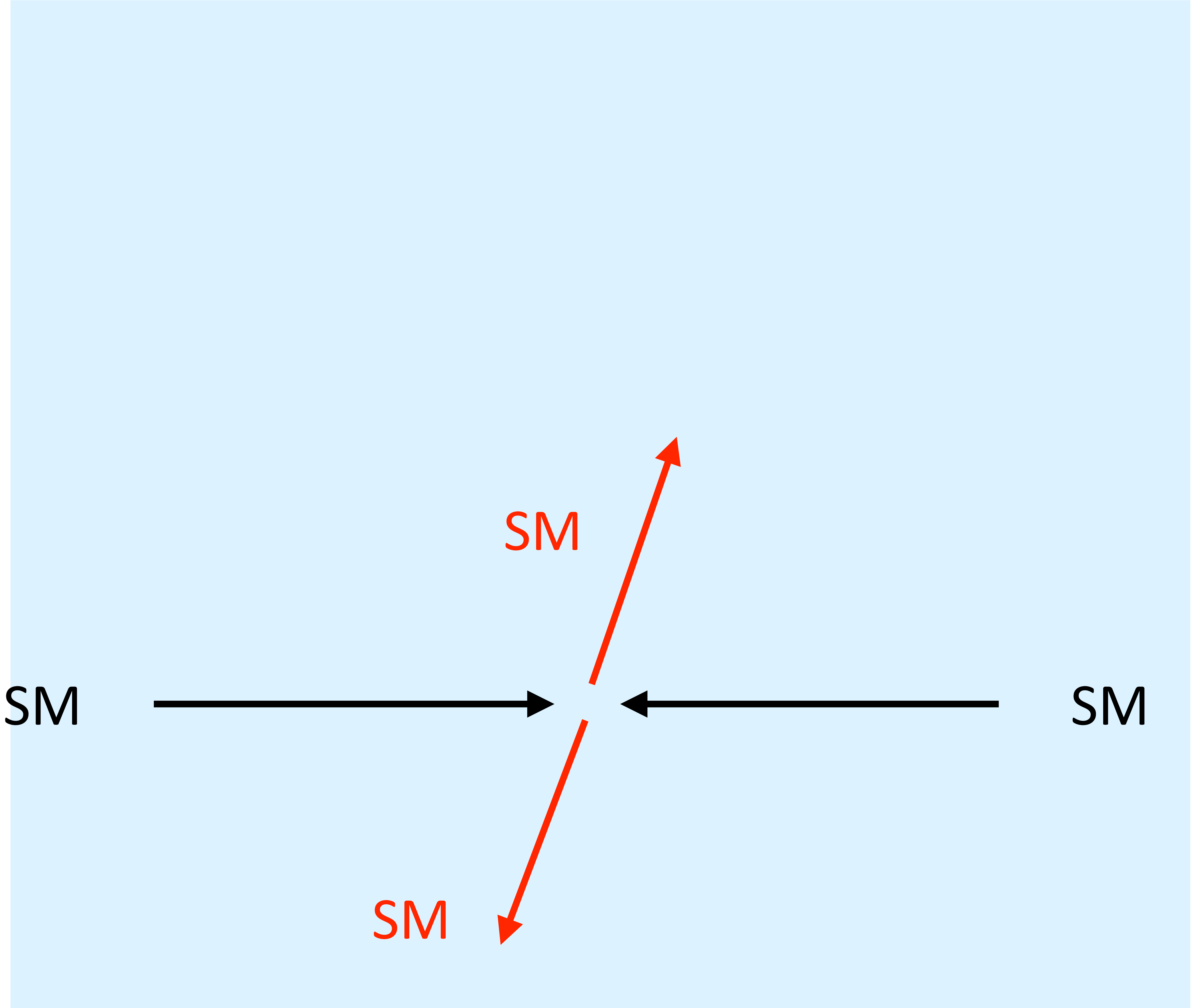

A pair of SM particles
produced at the primary vertex

We propose a new dark matter channel at colliders

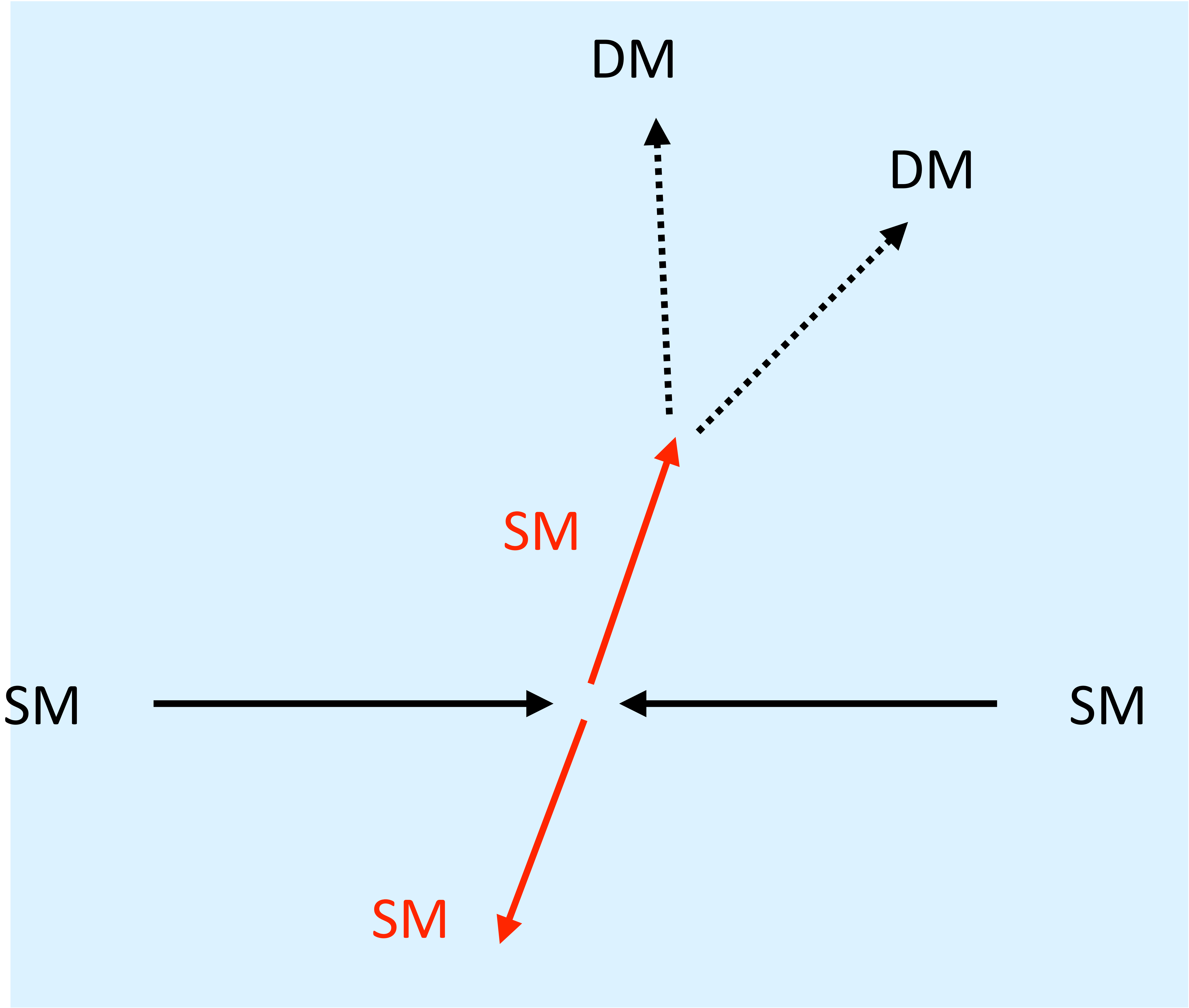

One SM particle interacts with the detector to produce a pair of DM particles

A pair of SM particles produced at the primary vertex

We propose a new dark matter channel at colliders

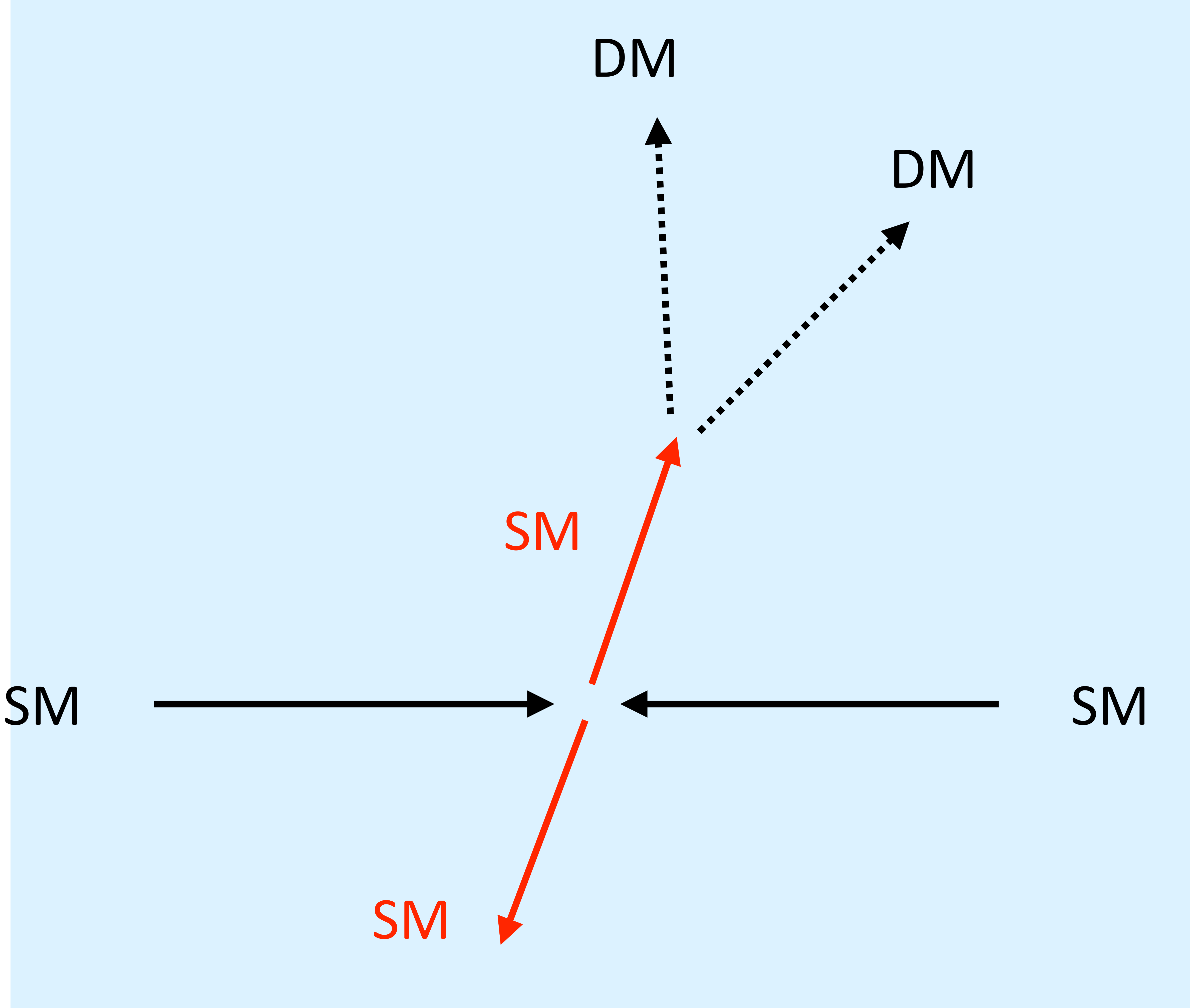

One SM particle interacts with the detector to produce a pair of DM particles

A pair of SM particles produced at the primary vertex

fixed target in collider

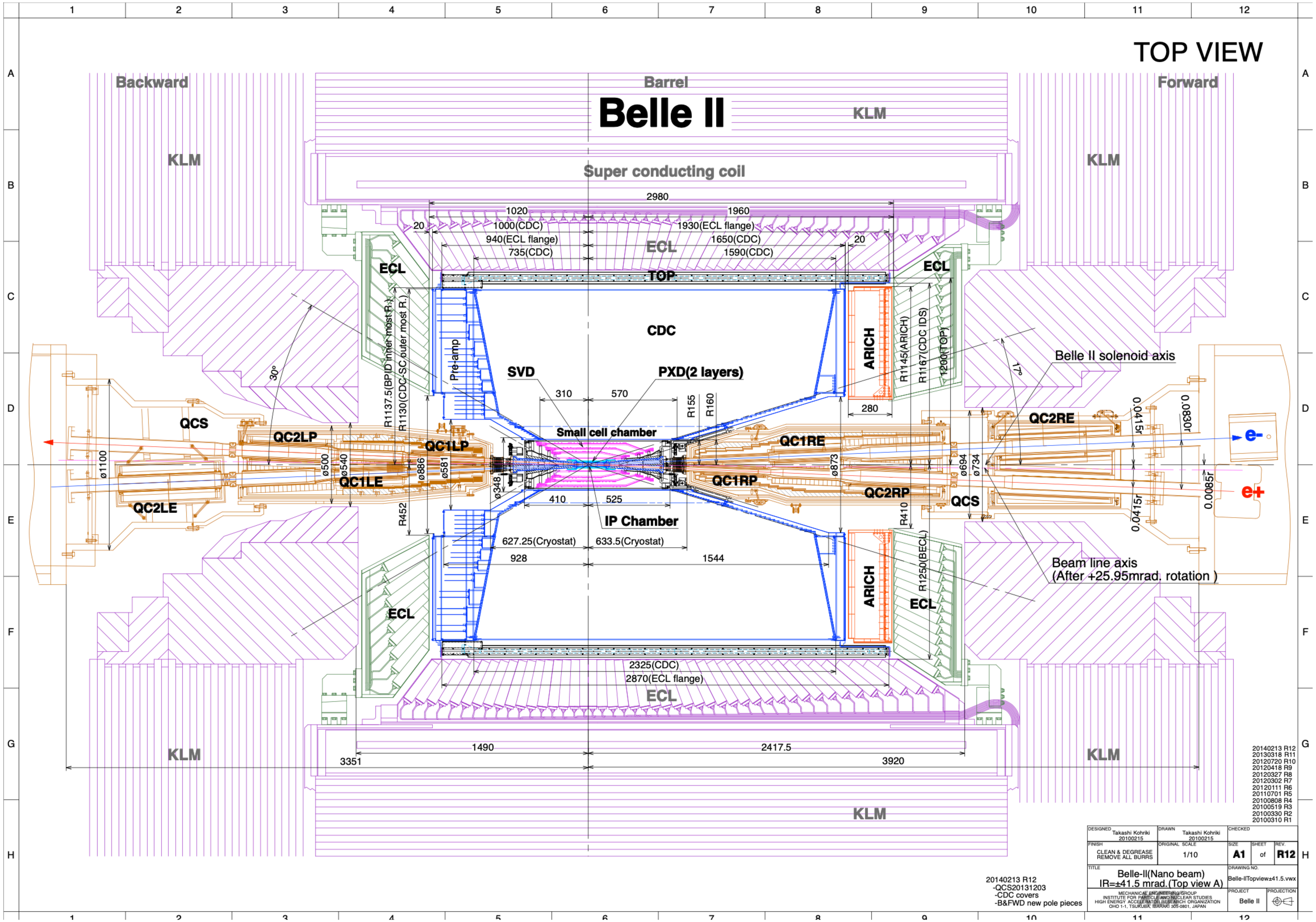
TOP VIEW
Backward
Barrel
Forward
Belle II
KLM
Super conducting coil
ECL
TOP
CDC
ARICH
SVD
PXD(2 layers)
Pre-amp
Small cell chamber
IP Chamber
QCS
QC2LP
QC1LP
QC1LE
QC2LE
QC1RE
QC1RP
QC2RE
QC2RP
Belle II solenoid axis
Beam line axis
(After +25.95mrad. rotation)
e-
e+
2980
1020
1960
1000(CDC)
1930(ECL flange)
940(ECL flange)
1650(CDC)
735(CDC)
1590(CDC)
20
R1137.5(BPID inner most R.)
R1130(CDC-SC outer most R.)
R1145(ARICH)
R1167(CDC IDS)
1200(TOP)
R1250(BECL)
R155
R160
R410
R452
310
570
410
525
280
627.25(Cryostat)
633.5(Cryostat)
928
1544
2325(CDC)
2870(ECL flange)
1490
2417.5
3351
3920
30°
17°
ø1100
ø500
ø540
ø886
ø581
ø348
ø873
ø694
ø734
0.0415r
0.0830r
0.0085r
20140213 R12
20130318 R11
20120720 R10
20120418 R9
20120327 R8
20120302 R7
20120111 R6
20110701 R5
20100808 R4
20100519 R3
20100330 R2
20100310 R1
20140213 R12
-QCS20131203
-CDC covers
-B&FWD new pole pieces
DESIGNED Takashi Kohriki 20100215
DRAWN Takashi Kohriki 20100215
CHECKED
FINISH CLEAN & DEGREASE REMOVE ALL BURRS
ORIGINAL SCALE 1/10
SIZE A1
SHEET of
REV. R12
TITLE Belle-II(Nano beam) IR=±41.5 mrad.(Top view A)
DRAWING NO. Belle-IITopview±41.5.vwx
MECHANICAL ENGINEERING GROUP
INSTITUTE FOR PARTICLE AND NUCLEAR STUDIES
HIGH ENERGY ACCELERATOR RESEARCH ORGANIZATION
OHO 1-1, TSUKUBA, IBARAKI 305-0801, JAPAN
PROJECT Belle II
PROJECTION

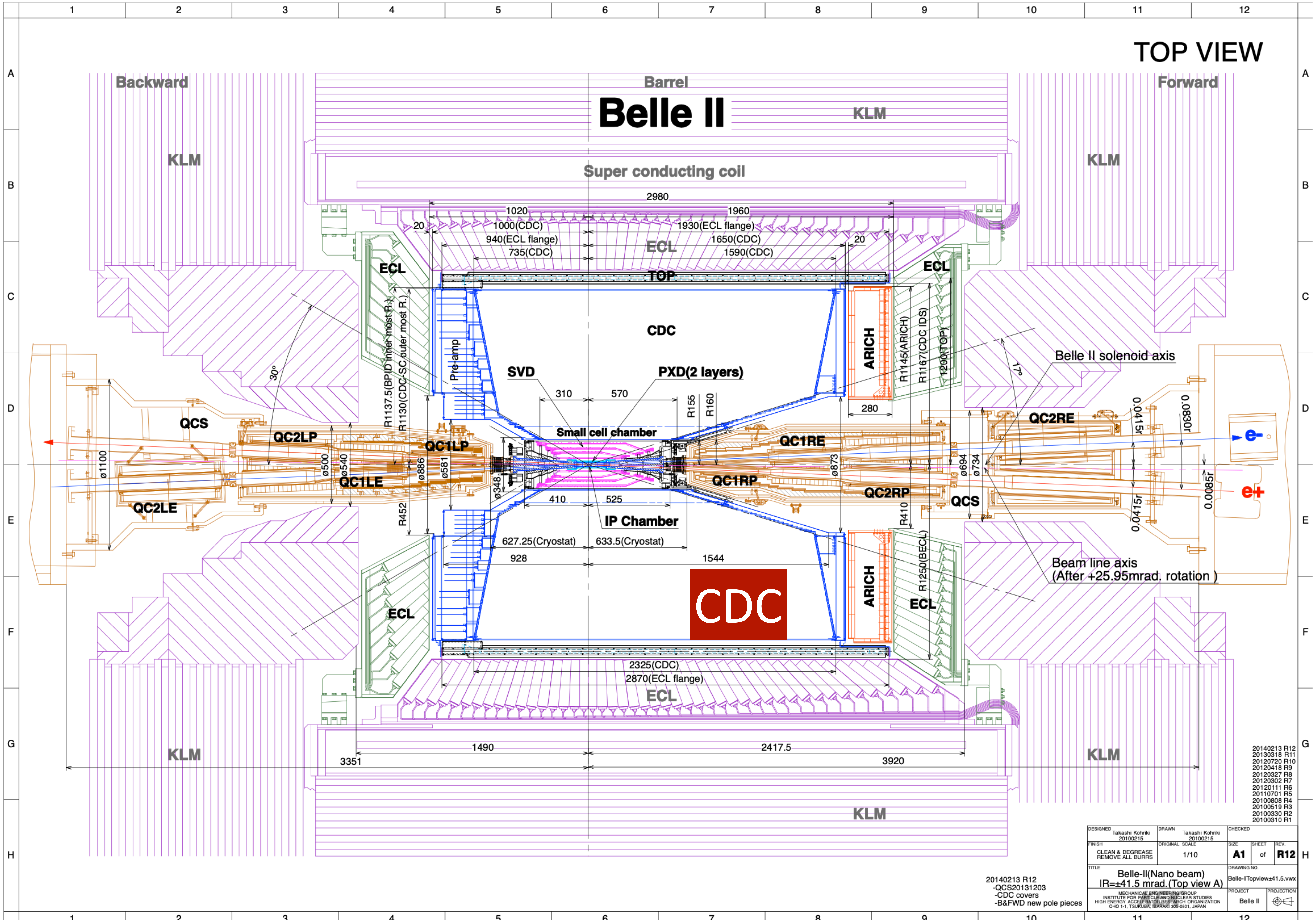

TOP VIEW
Backward
Barrel
Forward
Belle II
KLM
Super conducting coil
ECL
TOP
CDC
ARICH
SVD
PXD(2 layers)
Pre-amp
Small cell chamber
IP Chamber
QCS
QC2LP
QC1LP
QC1LE
QC2LE
QC1RE
QC1RP
QC2RE
QC2RP
Belle II solenoid axis
Beam line axis
(After +25.95mrad. rotation)
e-
e+
2980
1020
1960
1000(CDC)
1930(ECL flange)
940(ECL flange)
1650(CDC)
735(CDC)
1590(CDC)
20
310
570
410
525
280
627.25(Cryostat)
633.5(Cryostat)
928
1544
2325(CDC)
2870(ECL flange)
1490
2417.5
3351
3920
R1137.5(BPID inner most R.)
R1130(CDC-SC outer most R.)
R1145(ARICH)
R1167(CDC IDS)
1200(TOP)
R1250(BECL)
R452
R410
R155
R160
ø1100
ø500
ø540
ø886
ø581
ø348
ø873
ø694
ø734
30°
17°
0.0415r
0.0830r
0.0085r
Belle-II(Nano beam)
IR=±41.5 mrad.(Top view A)
Takashi Kohriki
1/10
A1
R12

CDC

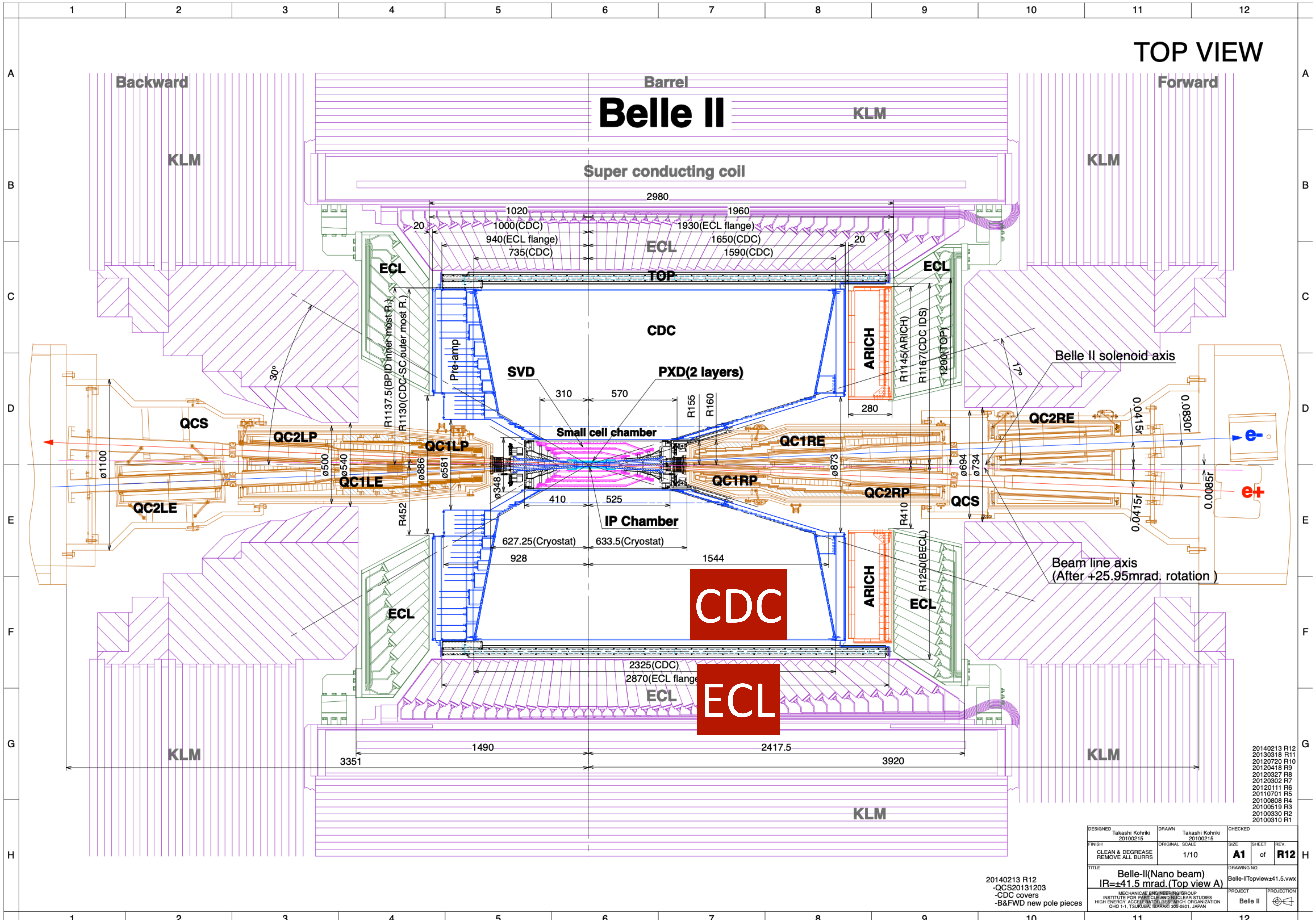

TOP VIEW
Backward
Barrel
Forward
Belle II
KLM
Super conducting coil
ECL
TOP
CDC
SVD
PXD(2 layers)
Pre-amp
Small cell chamber
IP Chamber
ARICH
QCS
QC2LP
QC1LP
QC1LE
QC2LE
QC2RE
QC1RE
QC1RP
QC2RP
Belle II solenoid axis
Beam line axis
(After +25.95mrad. rotation)
e-
e+
2980
1020
1960
1000(CDC)
1930(ECL flange)
940(ECL flange)
1650(CDC)
735(CDC)
1590(CDC)
20
310
570
410
525
R155
R160
280
R1137.5(BPID inner most R.)
R1130(CDC-SC outer most R.)
R1145(ARICH)
R1167(CDC IDS)
1200(TOP)
R1250(BECL)
R452
R410
30°
17°
ø1100
ø500
ø540
ø886
ø581
ø348
ø873
ø694
ø734
0.0415r
0.0830r
0.0085r
627.25(Cryostat)
633.5(Cryostat)
928
1544
2325(CDC)
2870(ECL flange)
1490
2417.5
3351
3920
CDC
ECL
Belle-II(Nano beam)
IR=±41.5 mrad.(Top view A)
Takashi Kohriki
20100215
1/10
A1
R12
20140213 R12
-QCS20131203
-CDC covers
-B&FWD new pole pieces

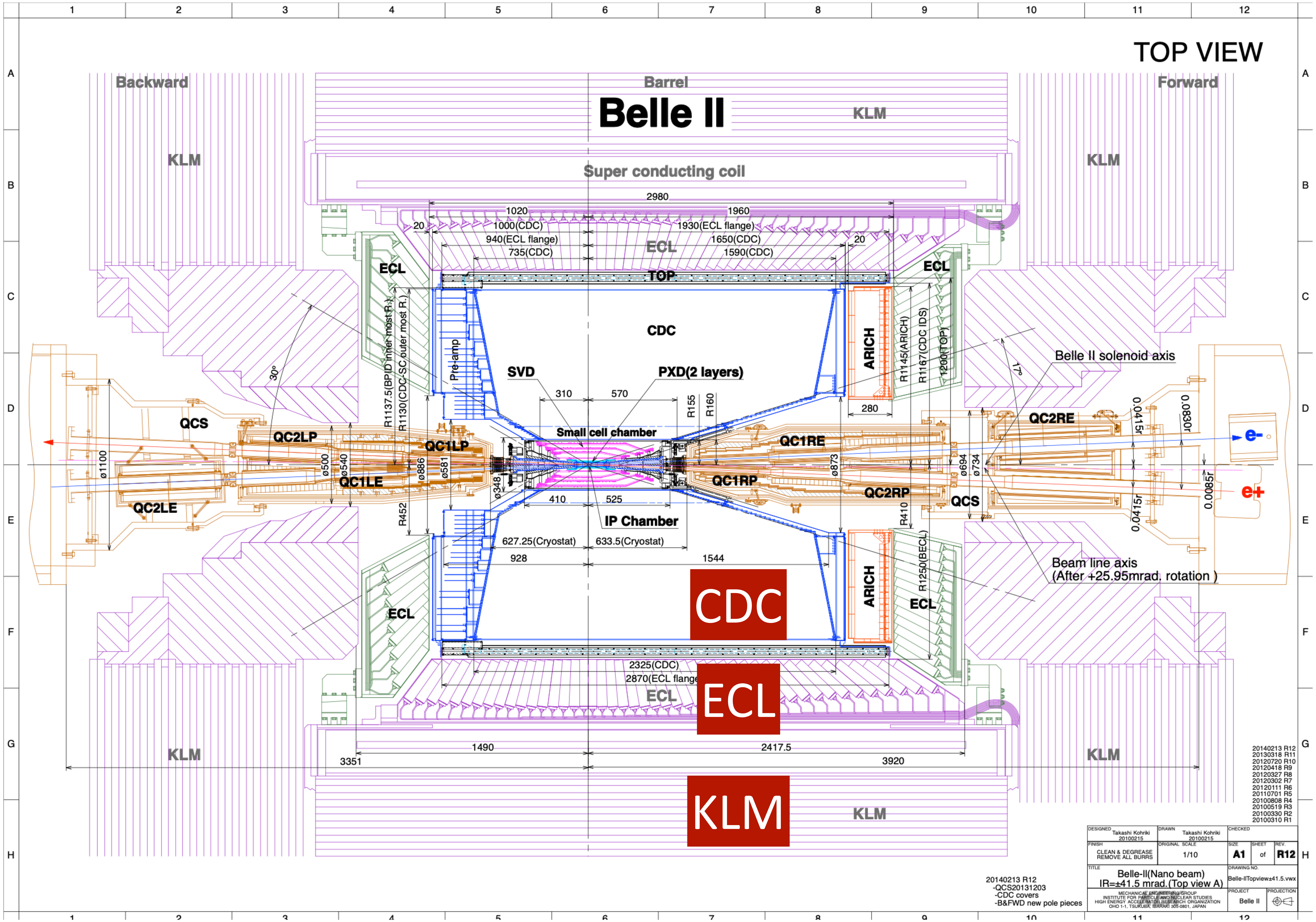
TOP VIEW
Backward
Barrel
Forward
Belle II
KLM
Super conducting coil
ECL
TOP
CDC
ARICH
SVD
PXD(2 layers)
Pre-amp
Small cell chamber
IP Chamber
QCS
QC2LP
QC1LP
QC1LE
QC2LE
QC1RE
QC1RP
QC2RE
QC2RP
Belle II solenoid axis
Beam line axis
(After +25.95mrad. rotation)
e-
e+
2980
1020
1960
1000(CDC)
1930(ECL flange)
940(ECL flange)
1650(CDC)
735(CDC)
1590(CDC)
310
570
410
525
627.25(Cryostat)
633.5(Cryostat)
928
1544
2325(CDC)
2870(ECL flange)
1490
2417.5
3351
3920
280
R1137.5(BPID inner most R.)
R1130(CDC-SC outer most R.)
R1145(ARICH)
R1167(CDC IDS)
R1200(TOP)
R1250(BECL)
R155
R160
R410
R452
ø1100
ø500
ø540
ø886
ø581
ø348
ø873
ø694
ø734
30°
17°
0.0415r
0.0830r
0.0085r
CDC
ECL
KLM
Belle-II(Nano beam)
IR=±41.5 mrad.(Top view A)
Takashi Kohriki
20100215
A1
R12
1/10
Belle II
20140213 R12
-QCS20131203
-CDC covers
-B&FWD new pole pieces

New DM channel @ Belle II (x-y plane)

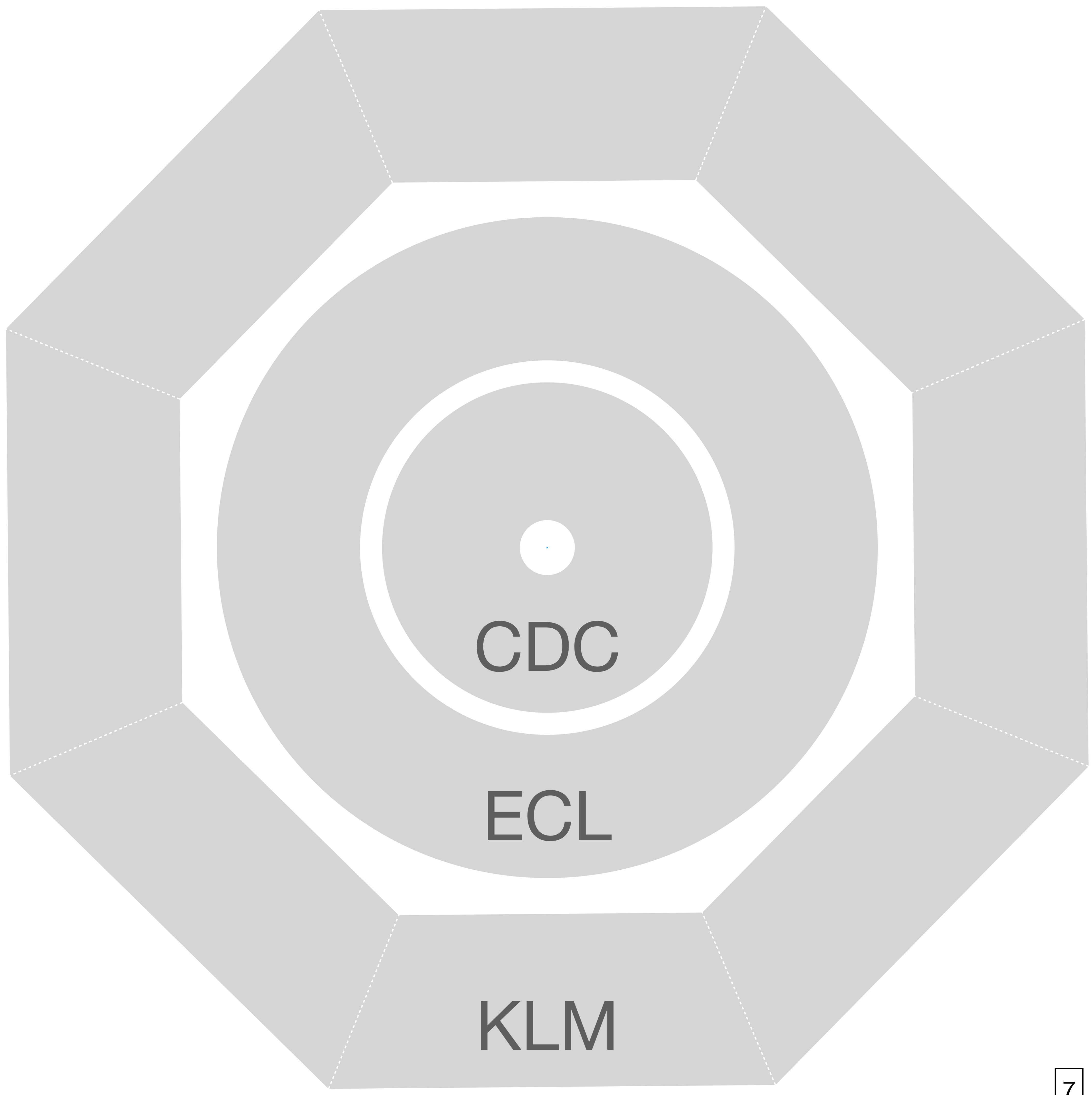

New DM channel @ Belle II (x-y plane)

$$e^+e^- \to e^+e^-$$

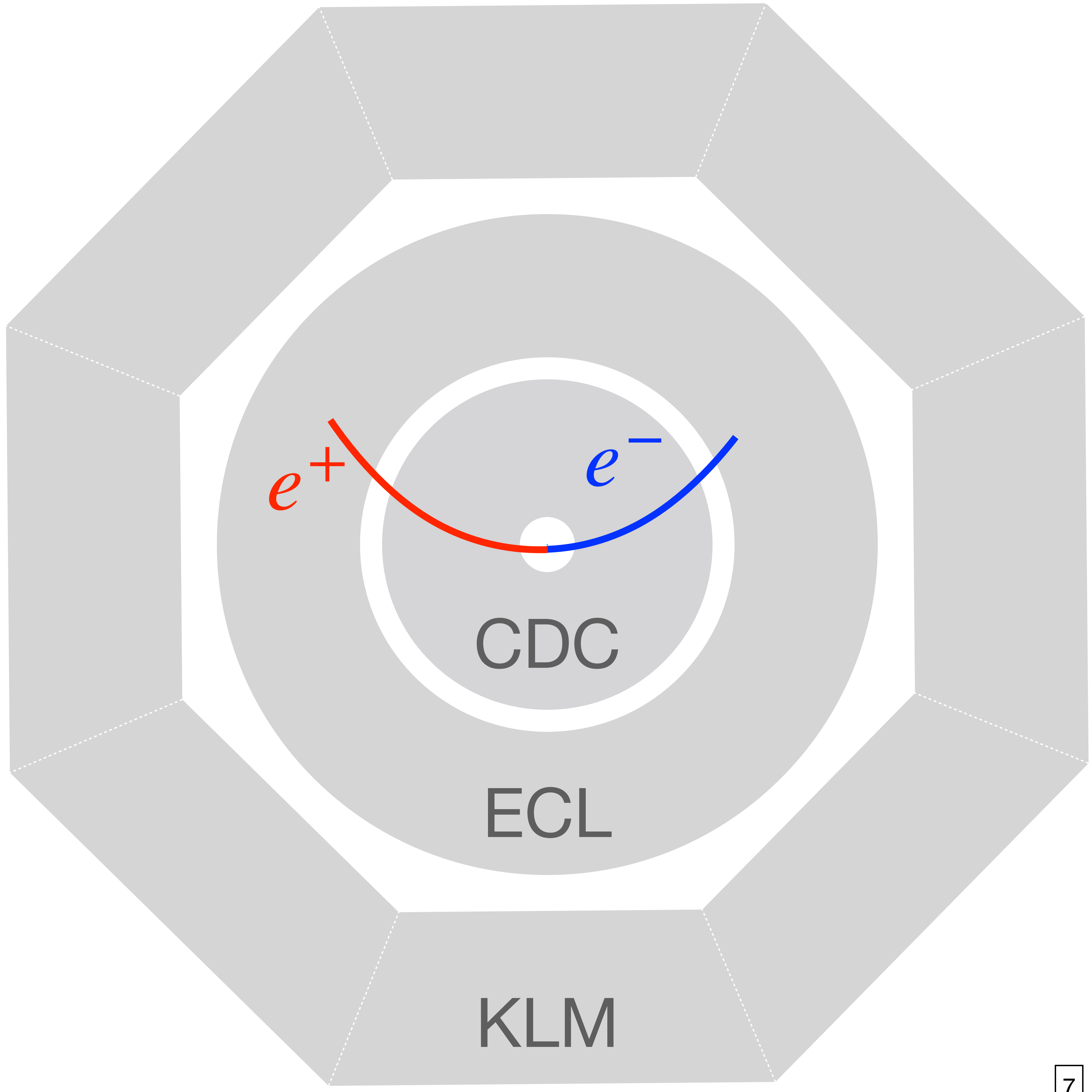

New DM channel @ Belle II (x-y plane)

$$e^+e^- \to e^+e^-$$

- e^- deposit energy in ECL

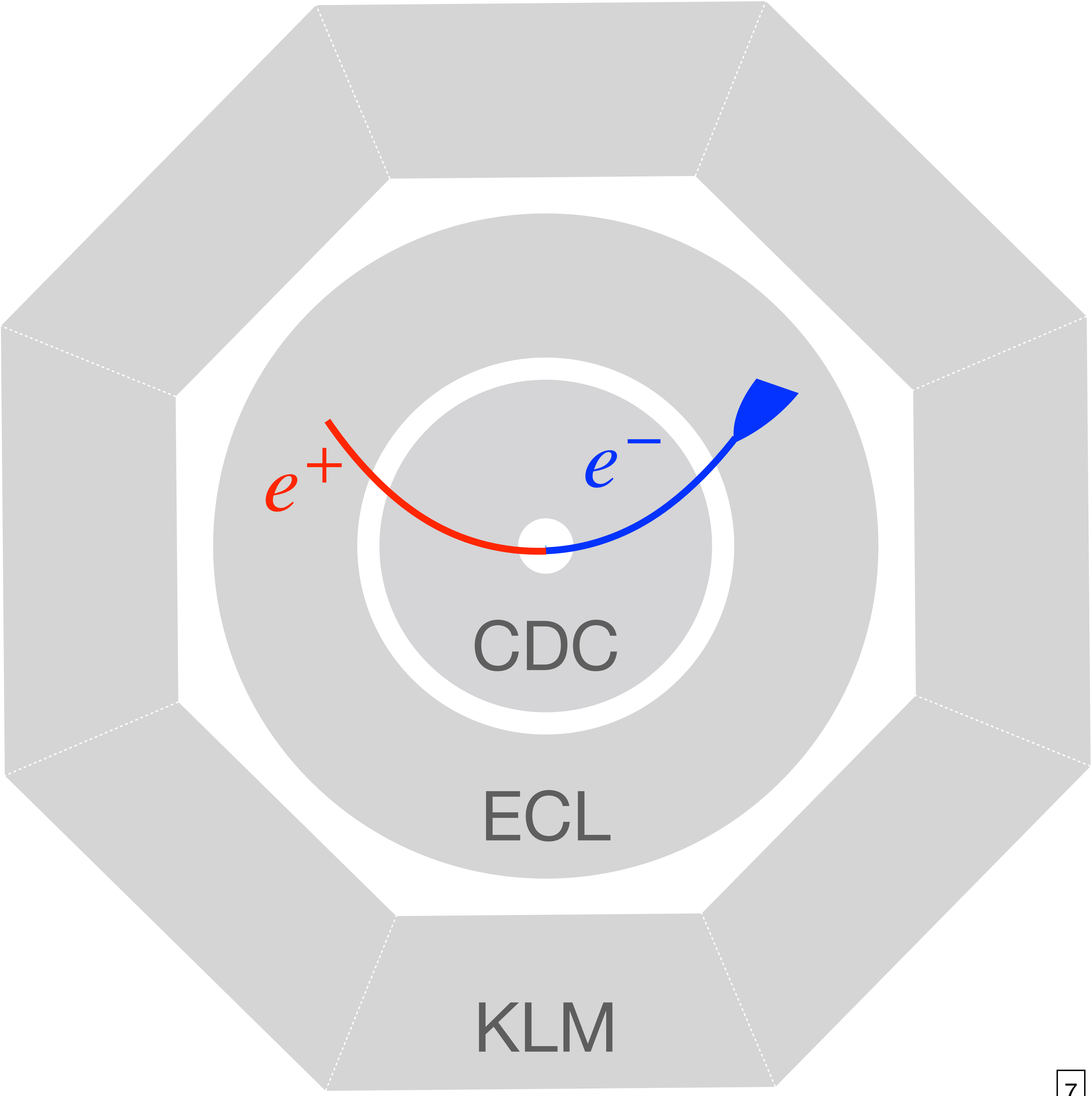

New DM channel @ Belle II (x-y plane)

$$e^+e^- \to e^+e^-$$

- e^- deposit energy in ECL
- e^+ interact with ECL to produce DM

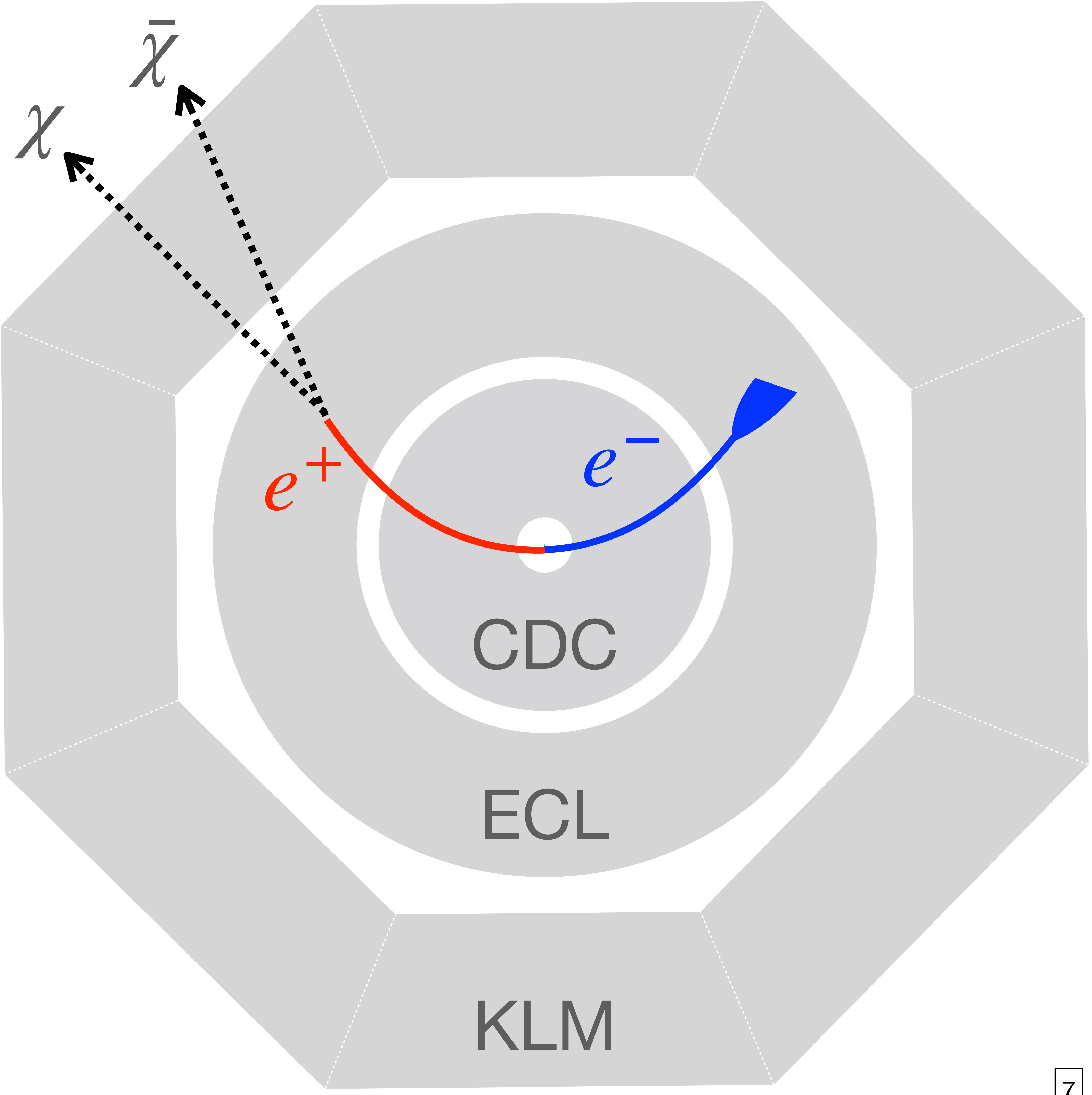

New DM channel @ Belle II (x-y plane)

$$e^+e^- \to e^+e^-$$

- e^- deposit energy in ECL
- e^+ interact with ECL to produce DM

disappearing positron track

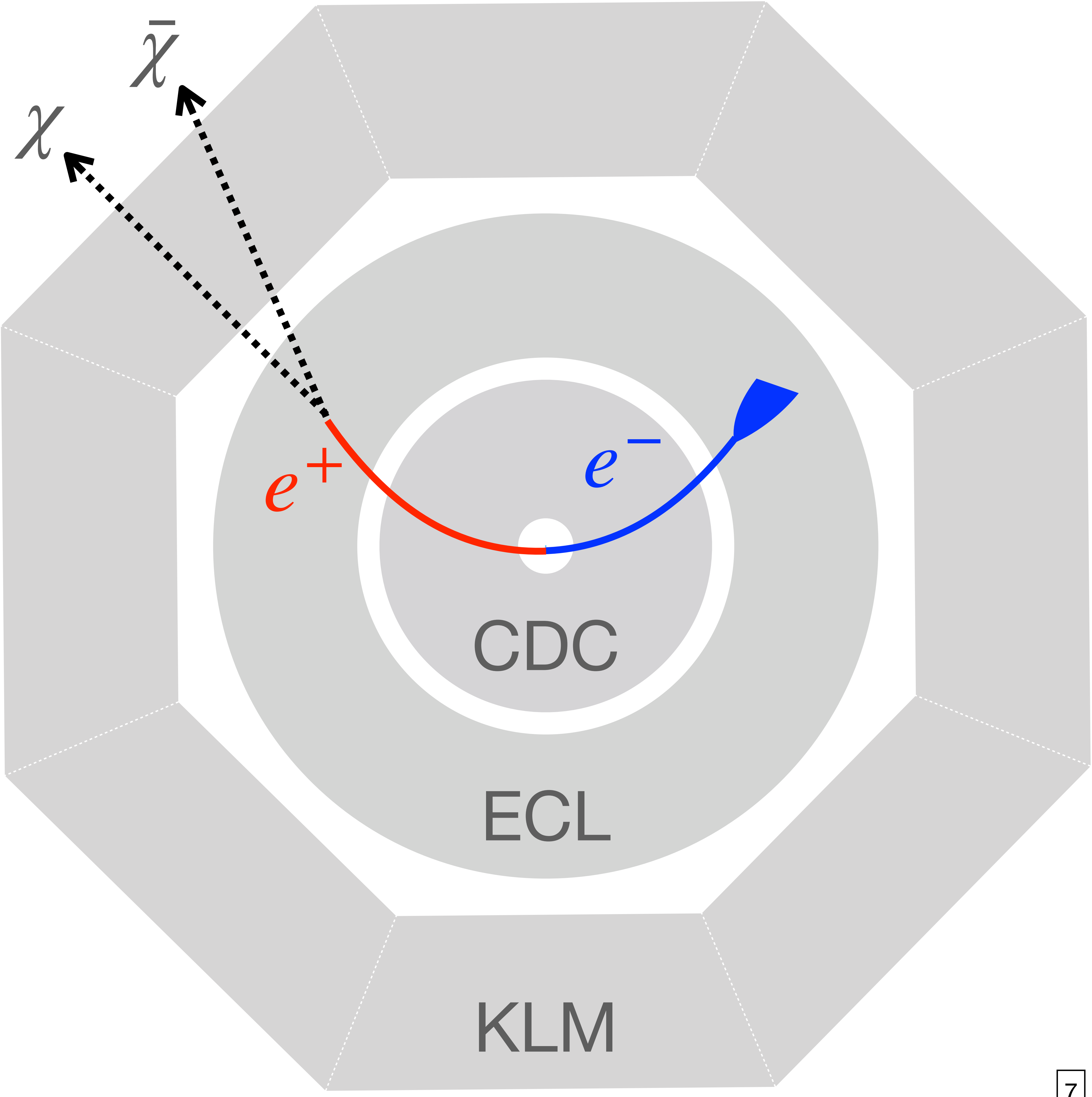

“disappearing positron track” signature

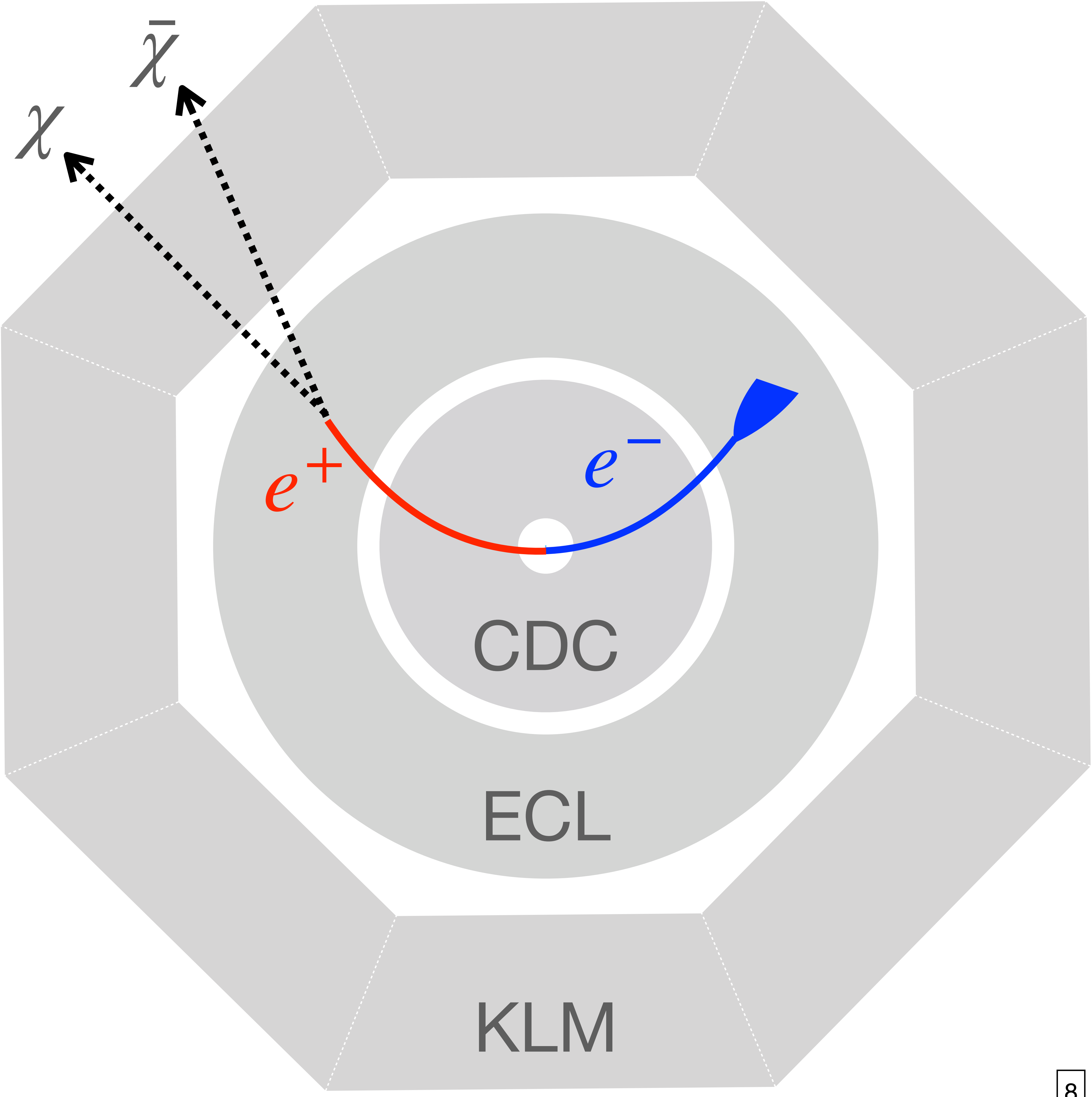

“disappearing positron track” signature

- CDC: e^- & e^+

CDC: $\dfrac{\delta p_T}{p_T} \simeq 0.4\,\%$ for $p_T \simeq 3$ GeV

Equal & opposite momenta
for e^- & e^+ in the CM frame

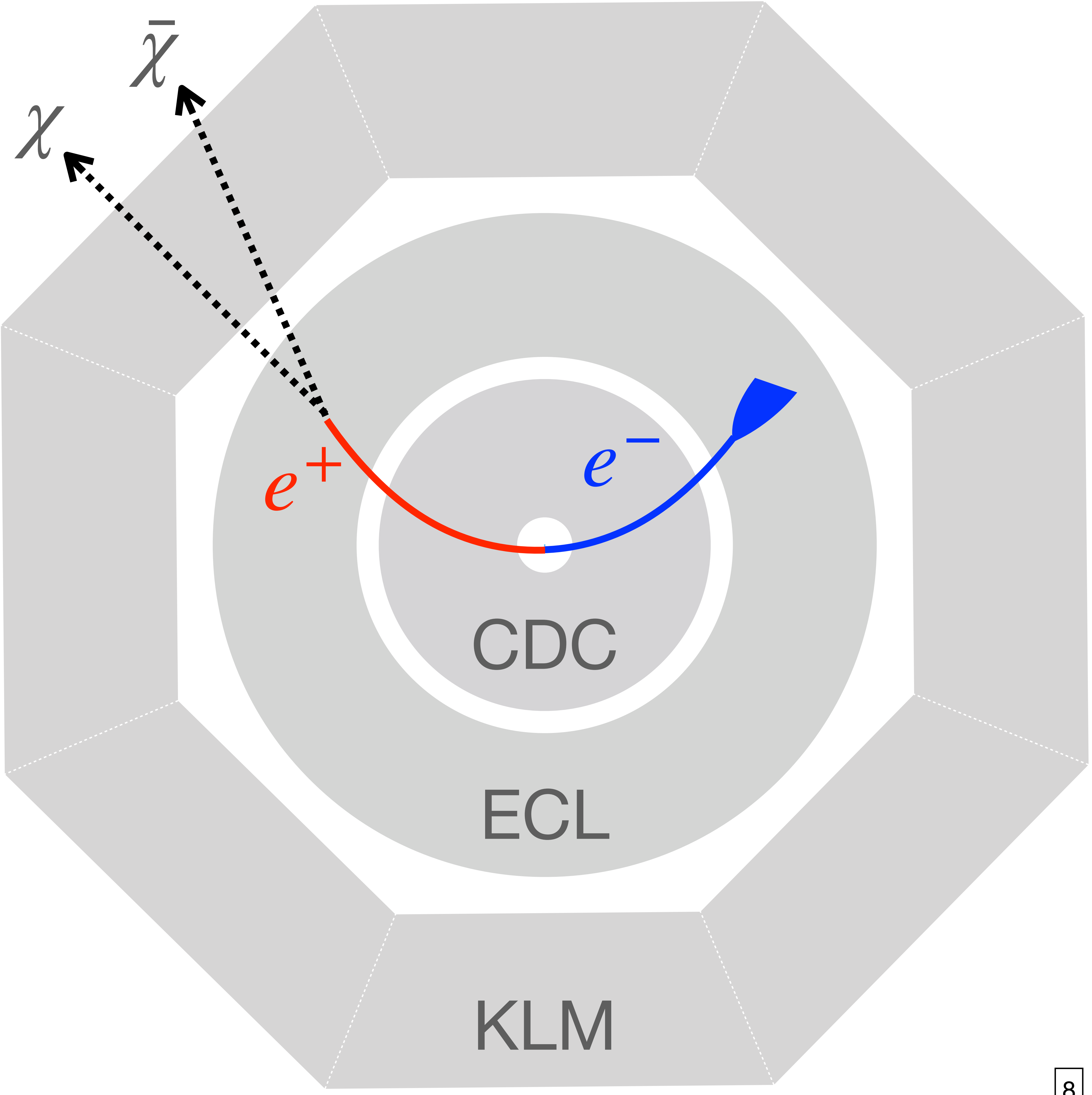

“disappearing positron track” signature

- CDC: e^- & e^+

  CDC: $\dfrac{\delta p_T}{p_T} \simeq 0.4\,\%$ for $p_T \simeq 3$ GeV

  Equal & opposite momenta for e^- & e^+ in the CM frame

- ECL: e^- & e^+

  missing energy: <5% e^+ energy in ECL

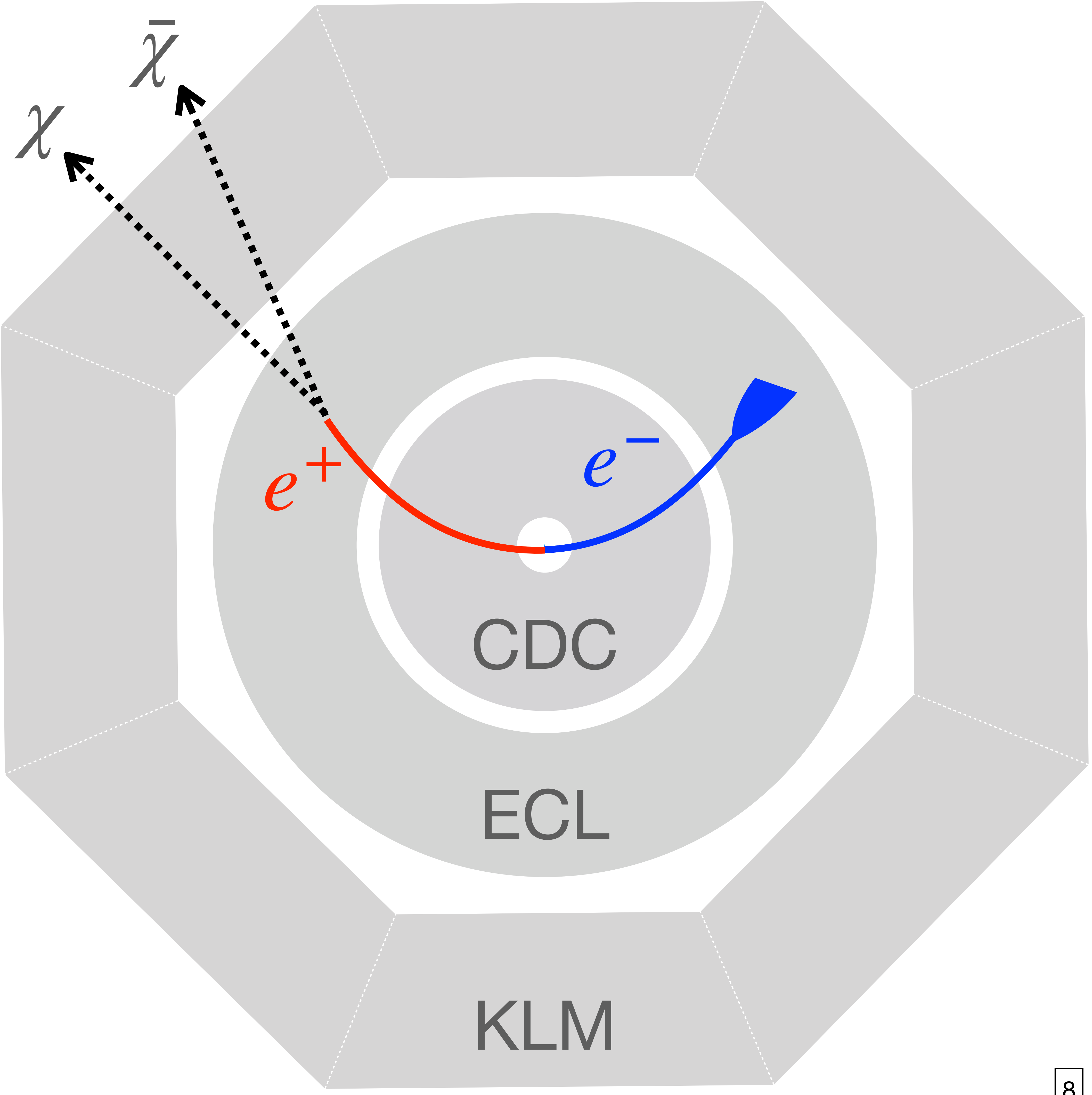

Use the ECL barrel region as the fixed target

ECL barrel: $32.2° < \theta < 128.7°$

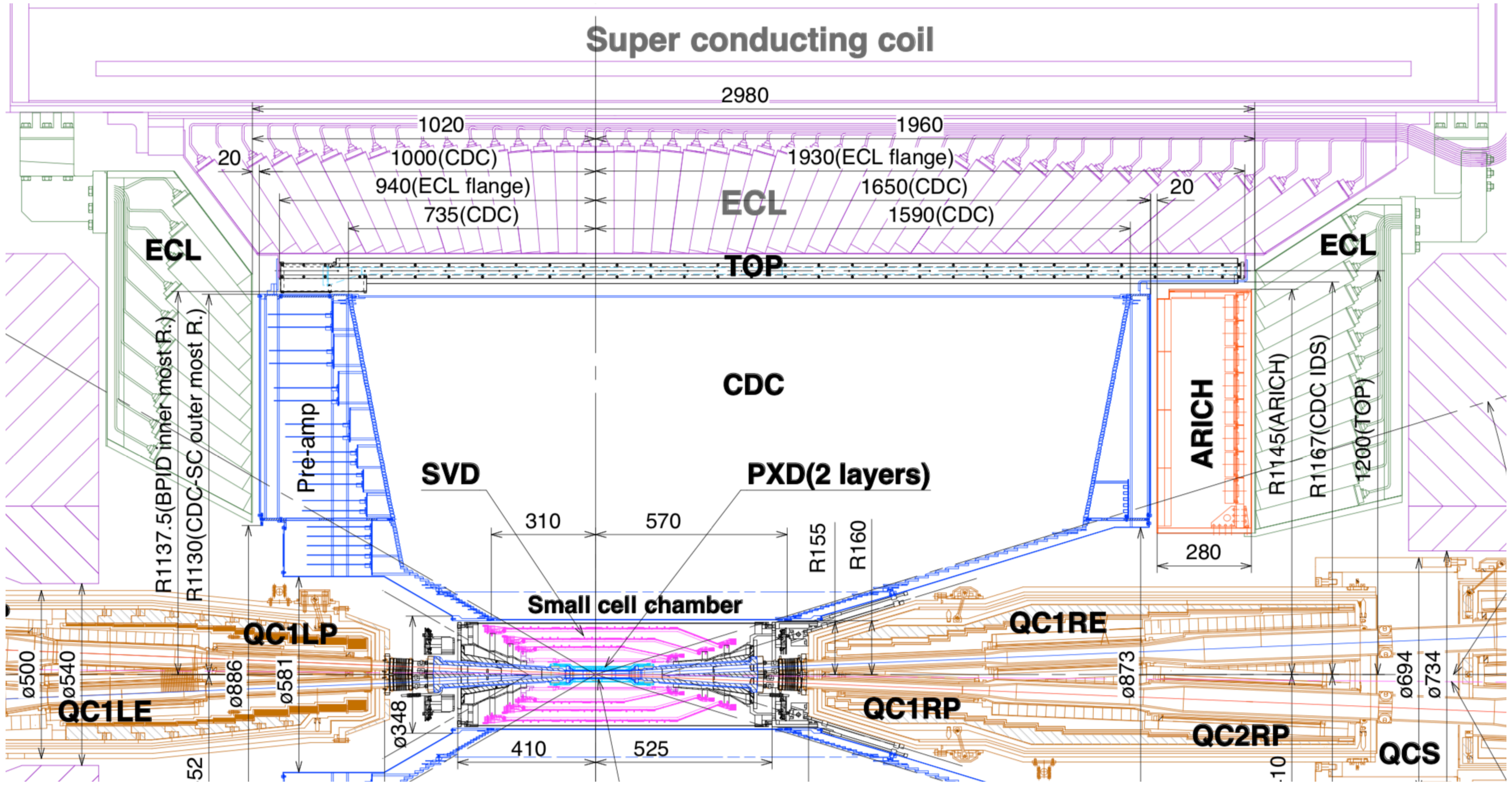

- Better hermiticity (non-projective gaps between ECL crystals)
- Less non-instrumented setups (e.g., magnetic wires) between ECL & KLM
- More beam BG in endcaps

$6 \times 10^{11}\ e^+e^-$ events from Bhabha scattering in the barrel region with 50/ab

Standard model backgrounds

Standard model backgrounds

BG: e^+ + ECL $\rightarrow \mathrm{SM}$

SM particles escape detection

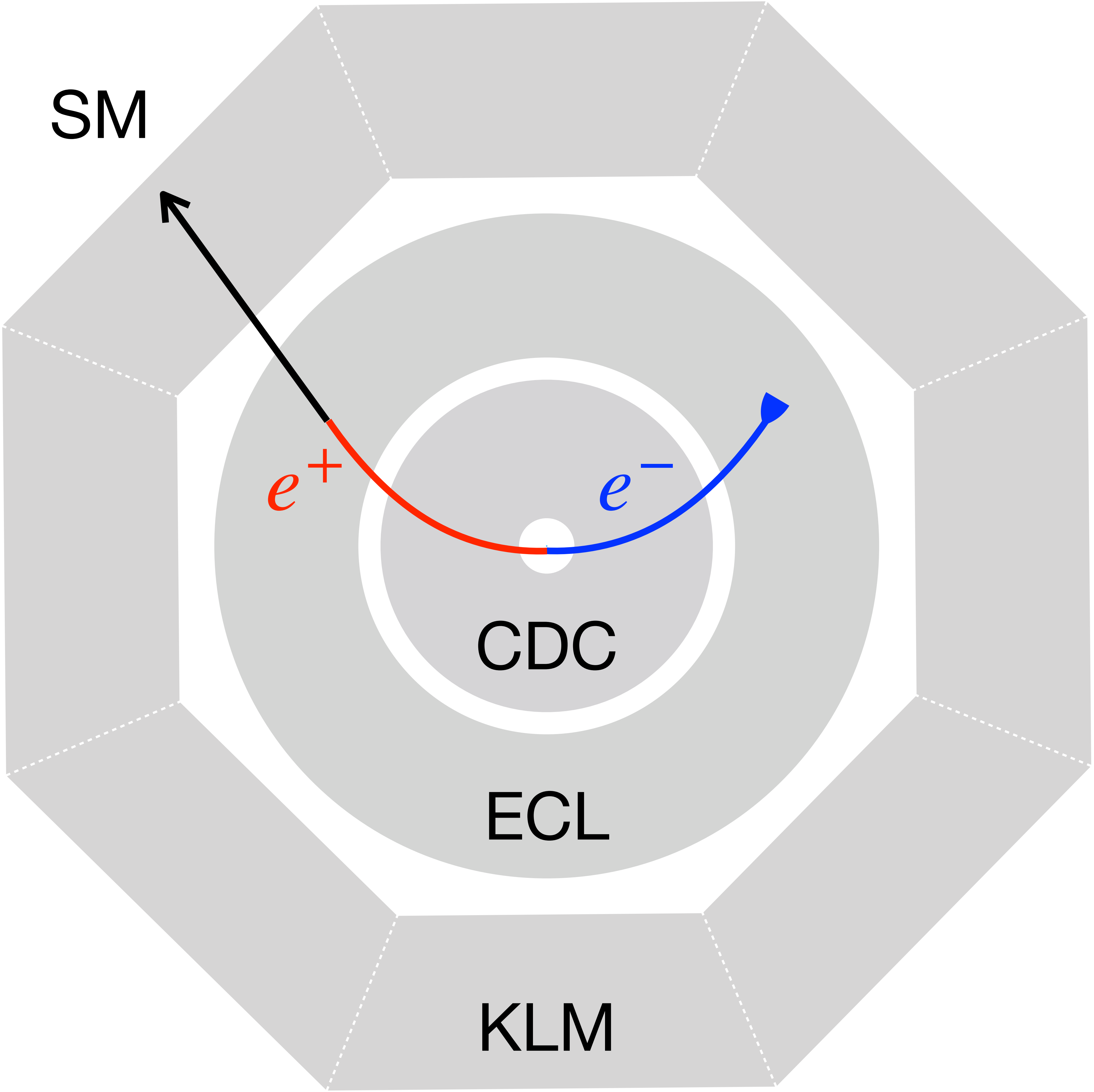

Standard model backgrounds

BG: e^+ + ECL $\rightarrow$ SM
SM particles escape detection

- Charged particles (e, μ, $\pi^{\pm}$): unlikely to contribute
- Neutral particles (n, γ, ν): neutrino BG is small
  main BG are due to n & γ

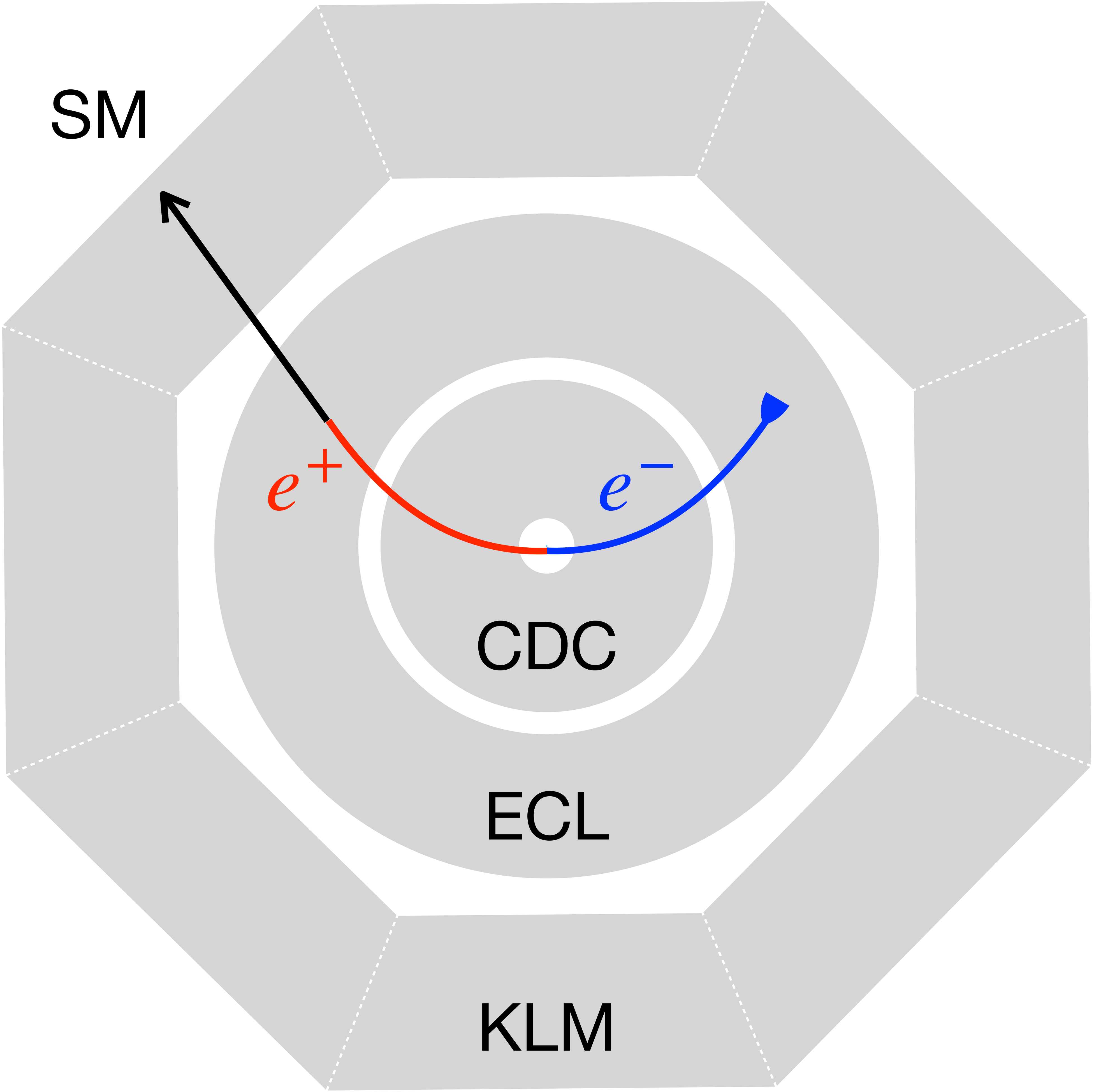

Photon-induced BG: high-E photons escape ECL

Photon spectrum (e^+ in matter) **[Tsai & Whitis 1966]**

$$\frac{dN_\gamma}{dx_\gamma}(t, x_\gamma) \simeq \frac{1}{x_\gamma}\frac{(1-x_\gamma)^{(4/3)t} - e^{-(7/9)t}}{7/9 + (4/3)\ln(1-x_\gamma)}$$

$x_\gamma = E_\gamma / E_e \qquad t = \#$ of X_0

ECL = 16-X_0 CsI crystals

prob of high-E γ = $\int_{0.95}^{1} dx_\gamma \frac{dN_\gamma}{dx_\gamma}(16, x_\gamma) \simeq 4.7 \times 10^{-8}$

# of high-E $\gamma \sim 2.8 \times 10^4$ after ECL (for 6×10^{11} incident e^+)

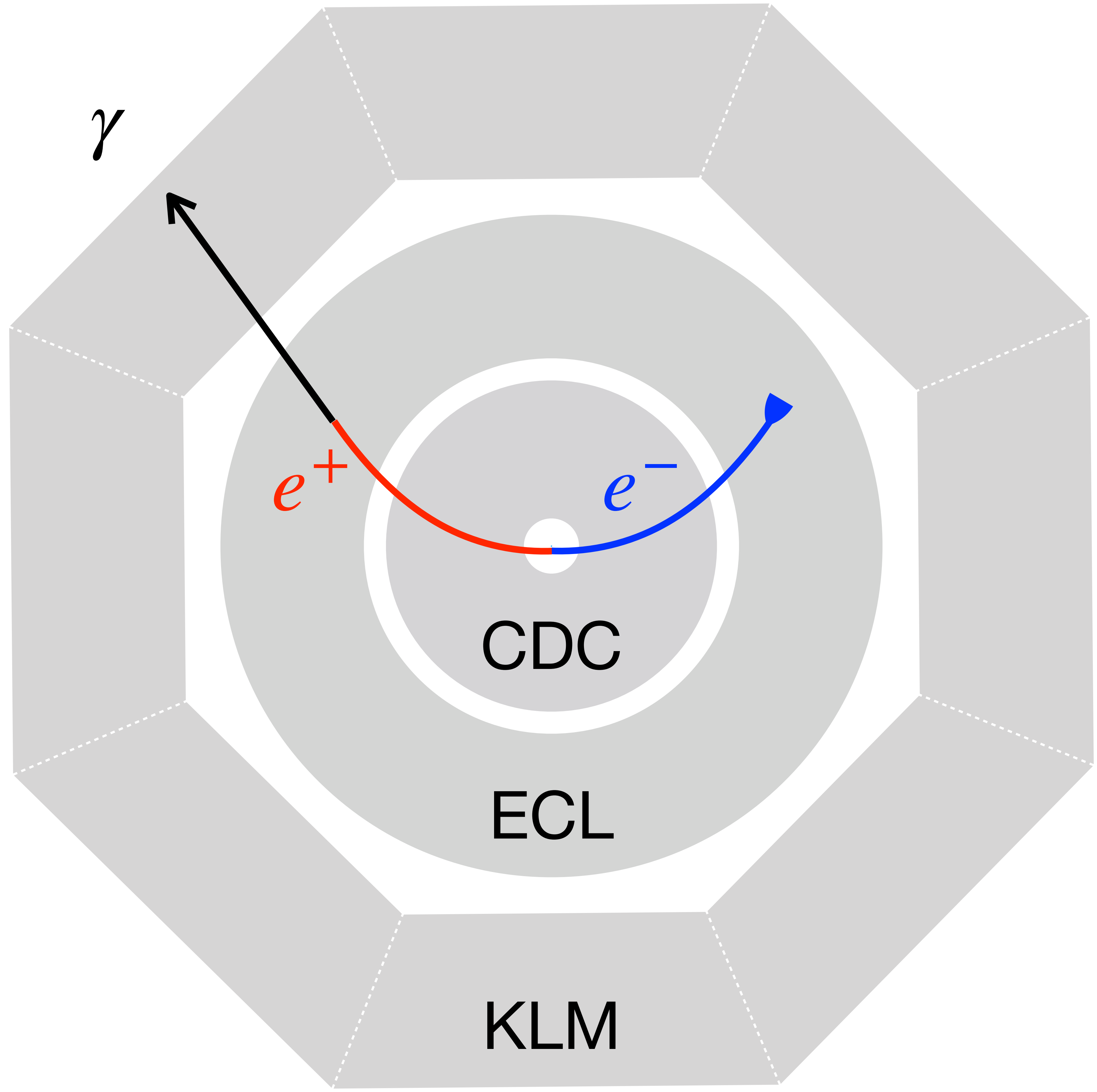

KLM veto capability on photon

KLM = alternating layers of 4.7-cm iron plates & active detectors $\Longrightarrow$ difficult for GeV γ to penetrate

However, γ can be absorbed by non-instrumented setups (e.g., magnet coil)

KLM veto efficiency = 4.5×10^{-4} (IFR @ BaBar)

13 photon BG (for 6×10^{11} incident e^+)

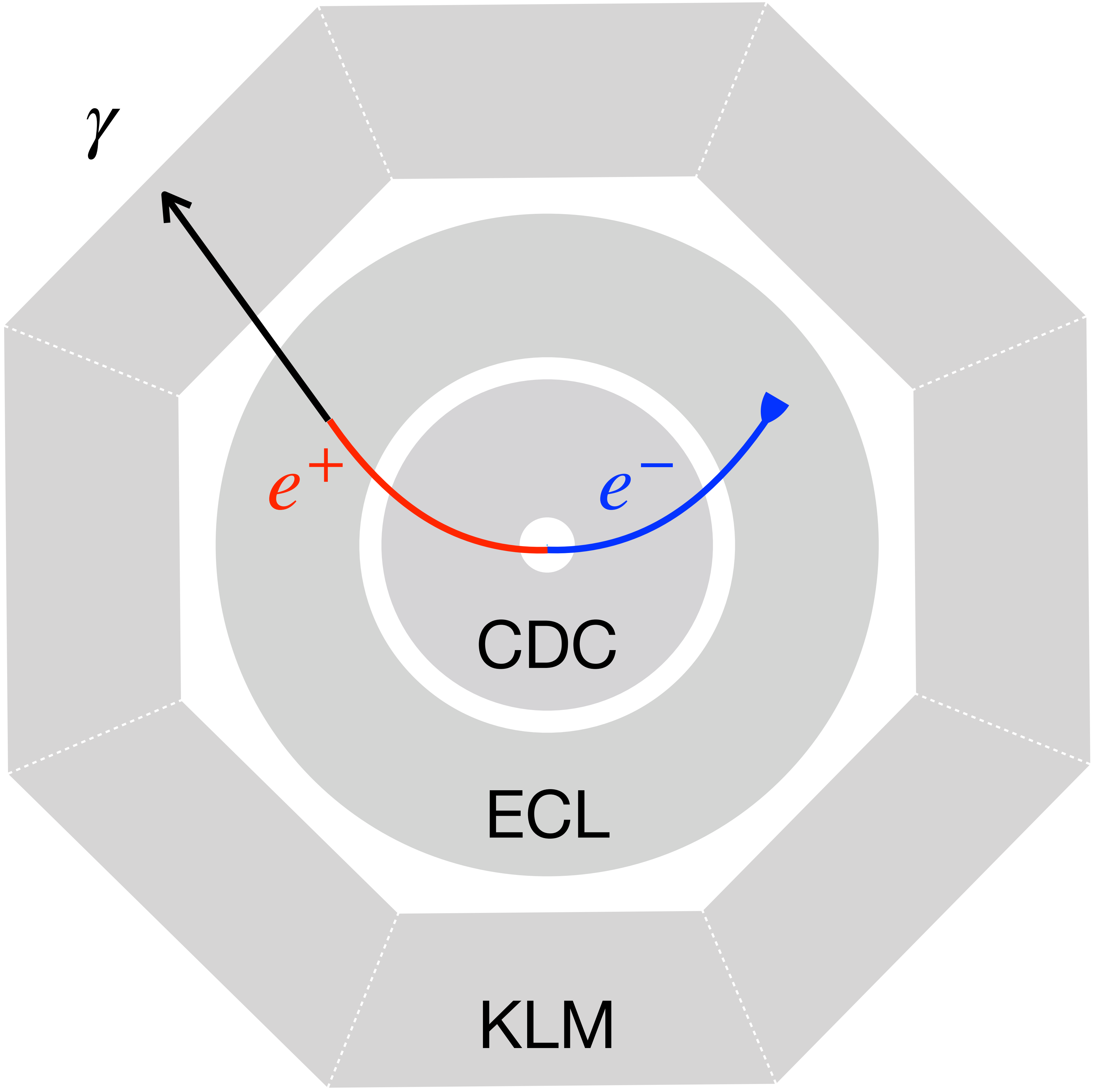

Neutron-induced backgrounds: GEANT4 simulations

GEANT4 simulation:
$10^9\ e^+$ with a CsI target w 1 X_0

Neutrons with significant energy are produced in the first X_0 (confirmed in simulations w 2 X_0)

At least one neutron with E > 3 GeV

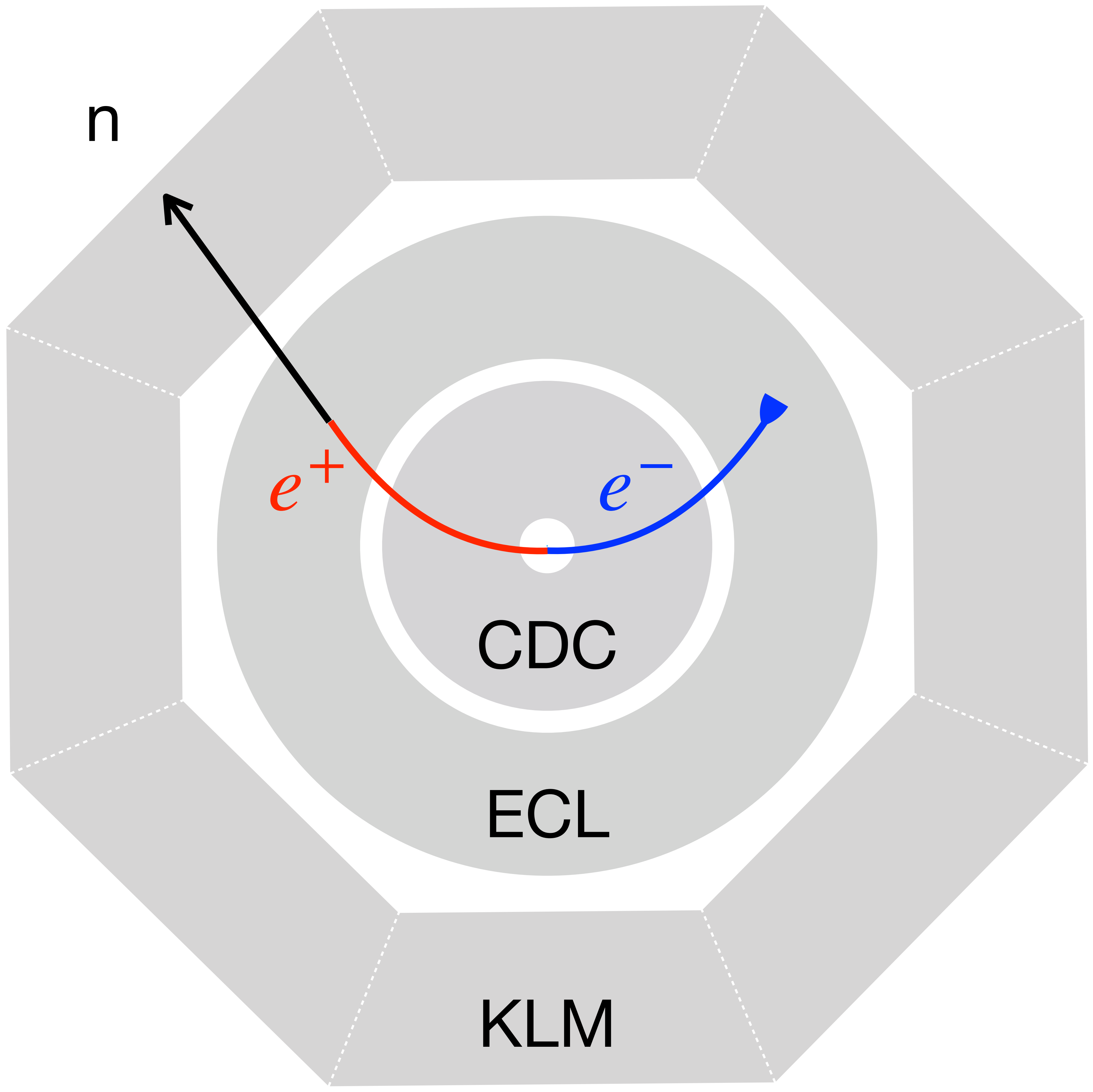

Probability for a neutron to penetrate ECL & KLM

Prob to penetrate a target with length L

$$P = \exp(-L/\lambda_0)$$

λ_0 = hadronic interaction length

KLM $\sim 3.9\,\lambda_0$ ECL $\sim 0.8\,\lambda_0$

Prob to penetrate ECL & KLM $\sim 1\,\%$

Neutron-induced BG $\sim\ 81$

Both photon & neutron-induced BG $\sim\ 94$

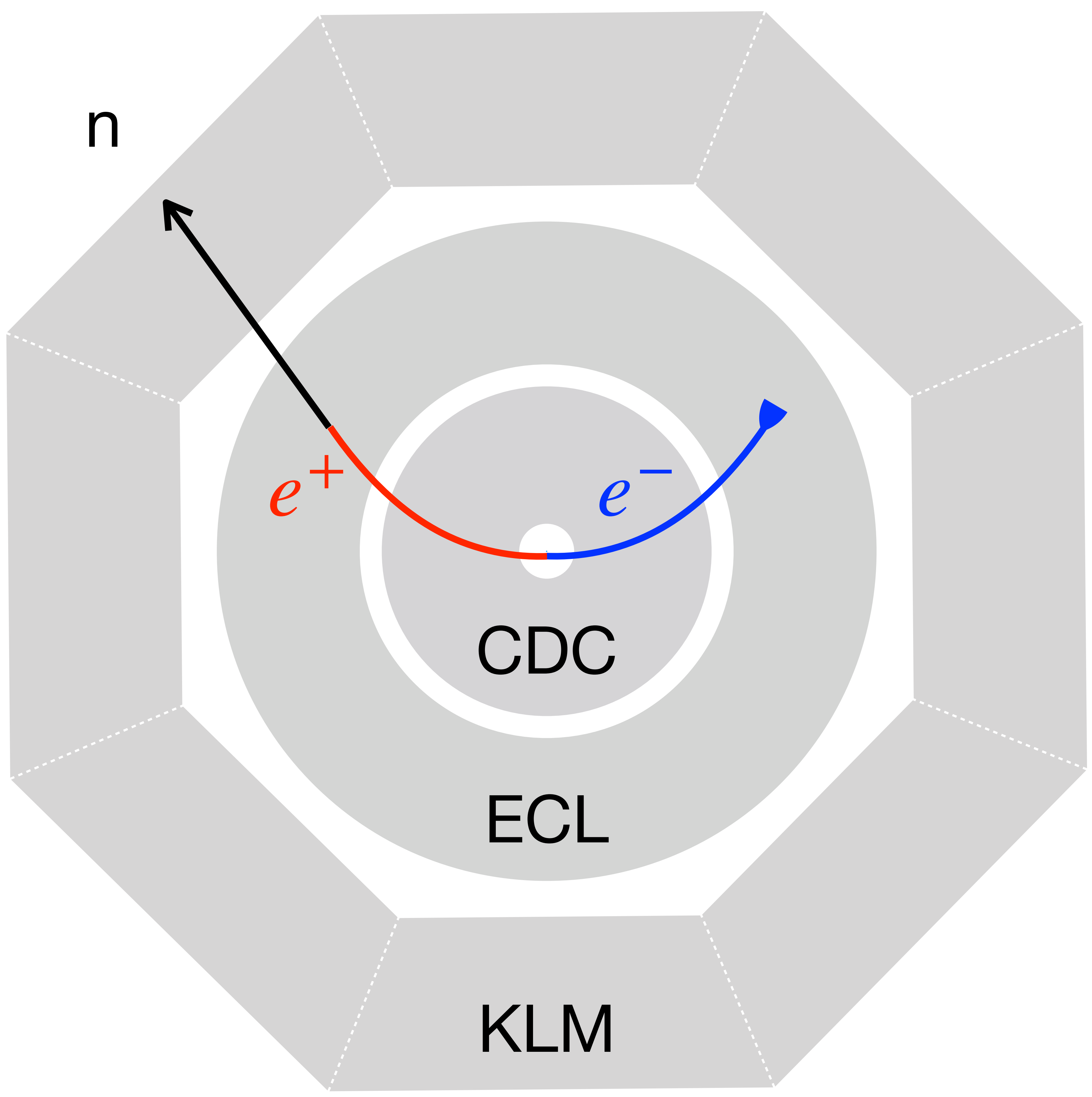

Sensitivity on invisible dark photon

Invisible dark photon

$$\delta B_{\mu\nu} X^{\mu\nu} \text{ or } m^2 \epsilon B_\mu X^\mu$$

$$\Downarrow$$

$$\mathscr{L}_{\text{int}} = A'_\mu (e Q_f \epsilon \bar{f} \gamma^\mu f + g_\chi \bar{\chi} \gamma^\mu \chi)$$

[Holdom 1986]

[Foot & He 1991]

[Feldman, ZL, Nath, hep-ph/0702123, 391 cites]

dark photon A'_μ

couplings: $g_\chi \gg e\epsilon$

$m_{A'} = 3 m_\chi$

⇨ invisible decay dominates

Positron interaction with ECL

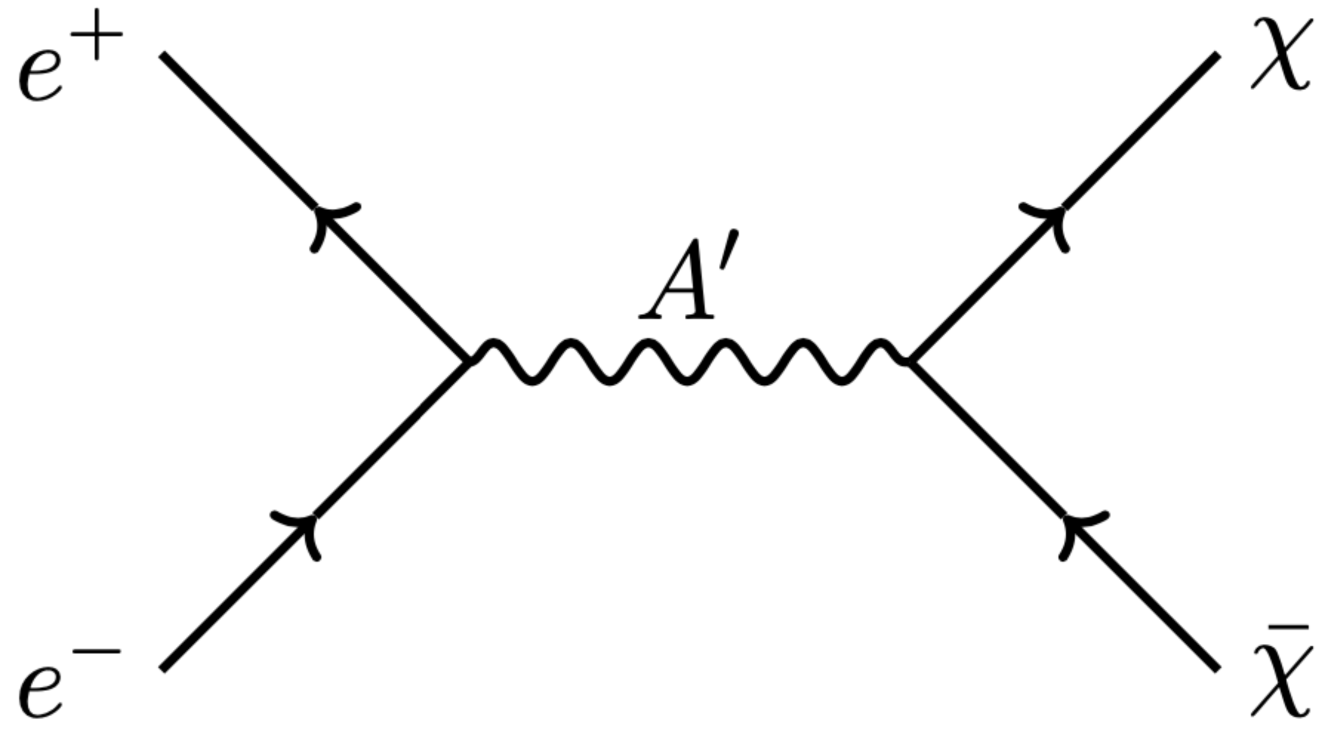

annihilation w/
atomic electrons

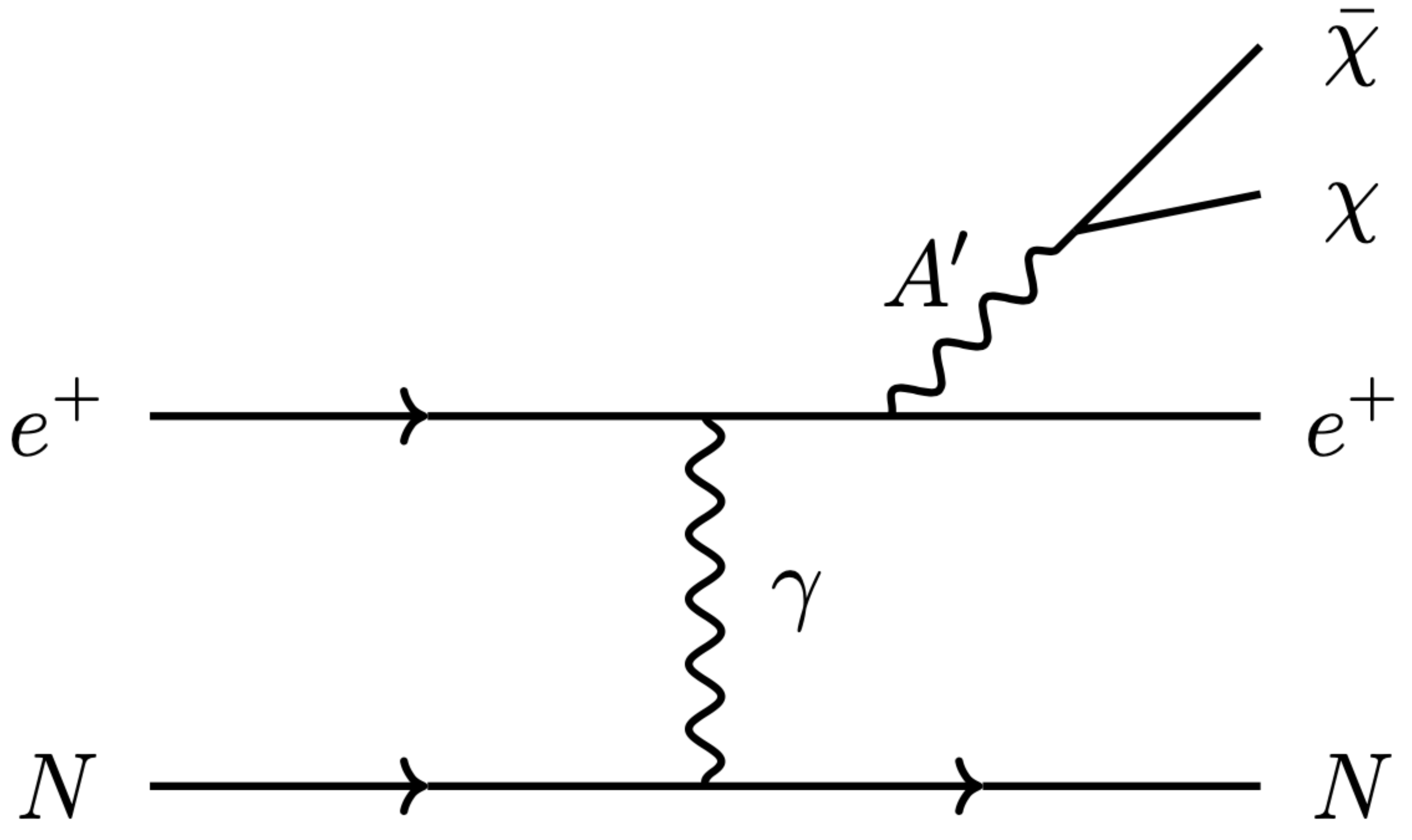

bremsstrahlung w/
target nucleus

Annihilation with atomic electrons

$$N_{\mathrm{ann}} = \mathscr{L} \int_{E_{\mathrm{min}}}^{E_{\mathrm{max}}} dE \frac{d\sigma_B}{dE} \int_{0.95E}^{E+m_e} dE_{A'}\, n_e\, T_e(E' = E_{A'} - m_e, E, L_T)\, \sigma_{\mathrm{ann}}(E_{A'})$$

- σ_B is the Bhabha xsec
- σ_{ann} is the annihilation xsec
- n_e is the electron # density
- T_e is the positron differential track length

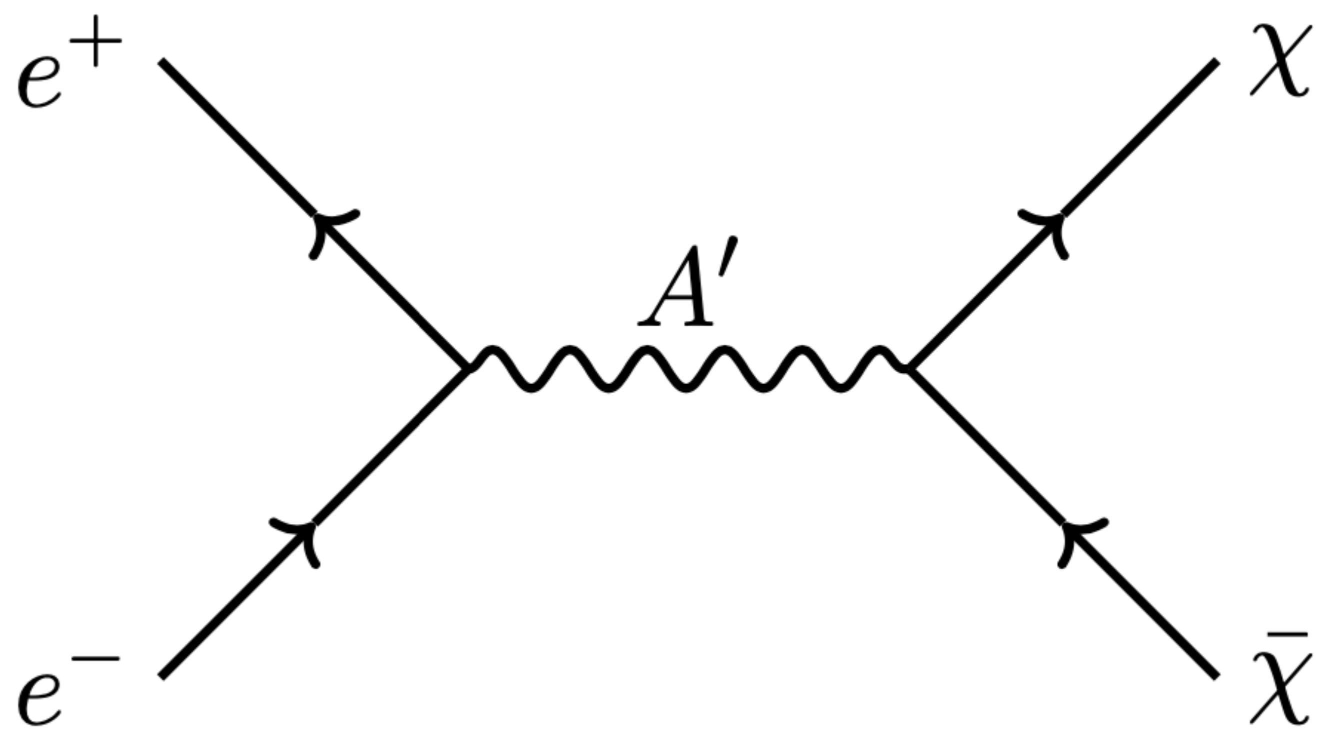

[Tsai & Whitis 1966]

Bremsstrahlung with target nucleus

$$N_{\rm bre} = \mathscr{L} \int_{E_{\rm min}}^{E_{\rm max}} dE \frac{d\sigma_B}{dE} \int_{0.95E}^{E-m_e} dE_{A'}\, n_N\, T_e(E', E, X_0)\, \frac{d\sigma_{\rm bre}}{dE_{A'}}$$

dominated by on-shell A' production

$\sigma_{\rm bre}$ is the xsec of on-shell produced A'

[Bjorken+ 0906.0580]
[Gninenko+ 1712.05706]
[Liu & Miller, 1705.01633]

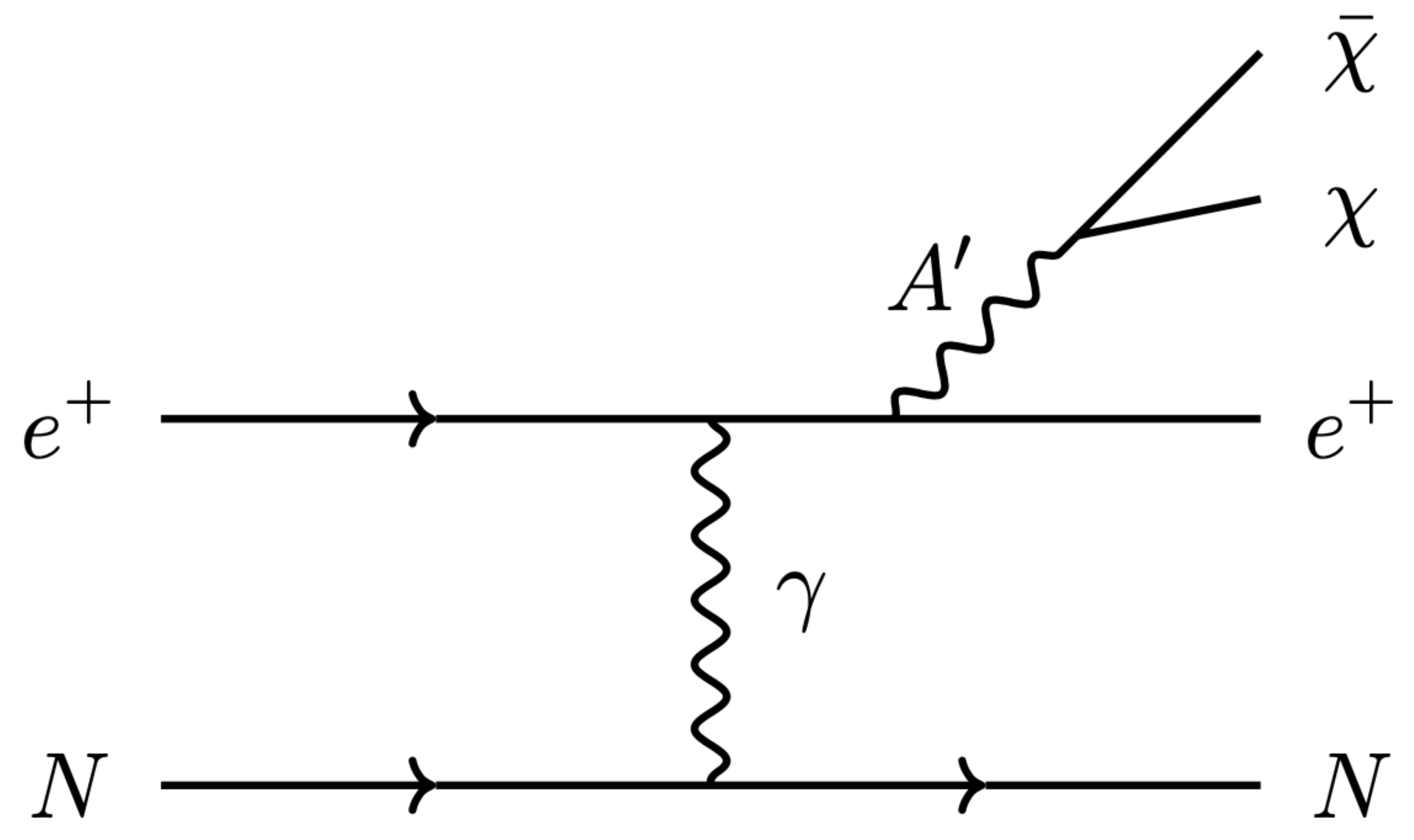

Belle II sensitivity on invisible dark photon

[Liang, ZL, Yang, 2212.04252]

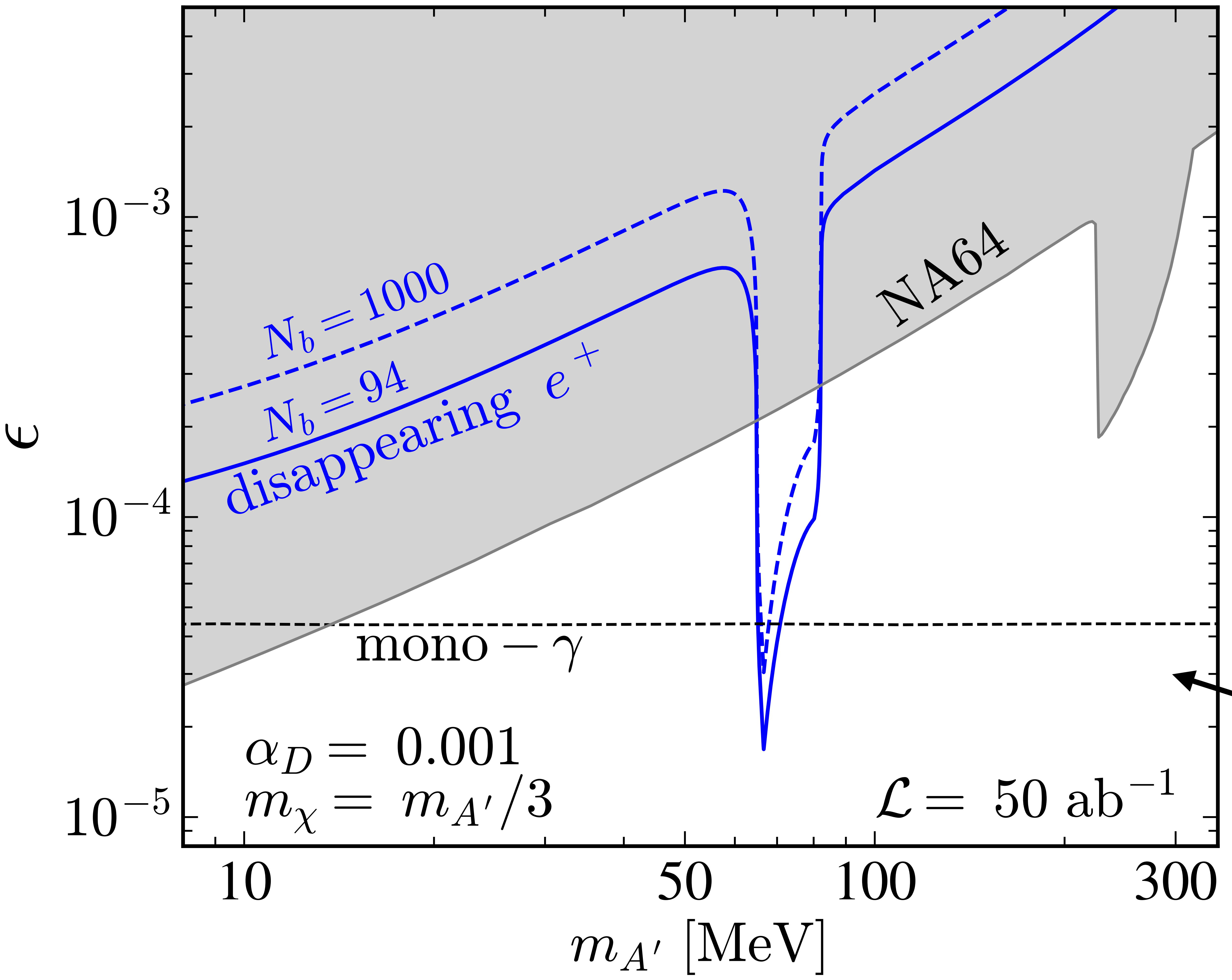

solid: 94 BG events

dashed: 1000 BG events

probing new parameter space beyond mono-photon and NA64

potential CRBG for DP m < 2 GeV [2207.06307]

2

Belle II probes of strongly-interacting dark matter

[Liang, ZL, Yang, PRD, 2312.08970]

Strongly interacting dark matter

DM is usually assumed to have a weak interaction w/ SM, e.g., WIMPs

However, strongly-interacting DM w/ a small abundance are allowed

DM gets boosted by various astro sources

- cosmic ray [Cappiello+, 1810.07705] [Bringmann+, 1810.10543] [Ema+, 1811.00520]
- diffuse supernova neutrino [Das+, 2104.00027]
- blazars [Wang+, 2111.13644]

Detection of strongly interacting DM can be difficult

strongly-interacting DM can be difficult to detect

- strong interaction xsec
- small abundance (because the strong interaction xsec)

- DMID: suppressed by the small abundance
- DMDD: suppressed by the small abundance & shielded by rock/air (like CR)
- CMB: unconstrained if the abundance is <0.4% **[Boddy +, 1808.00001]**

Colliders are ideal place to probe such DM, as they are not limited by these 2 factors.

Ceiling of collider searches

strongly-interacting DM starts to interacts w/ detectors ⇒ no more mono-X

[Cappiello+ 1810.07705]

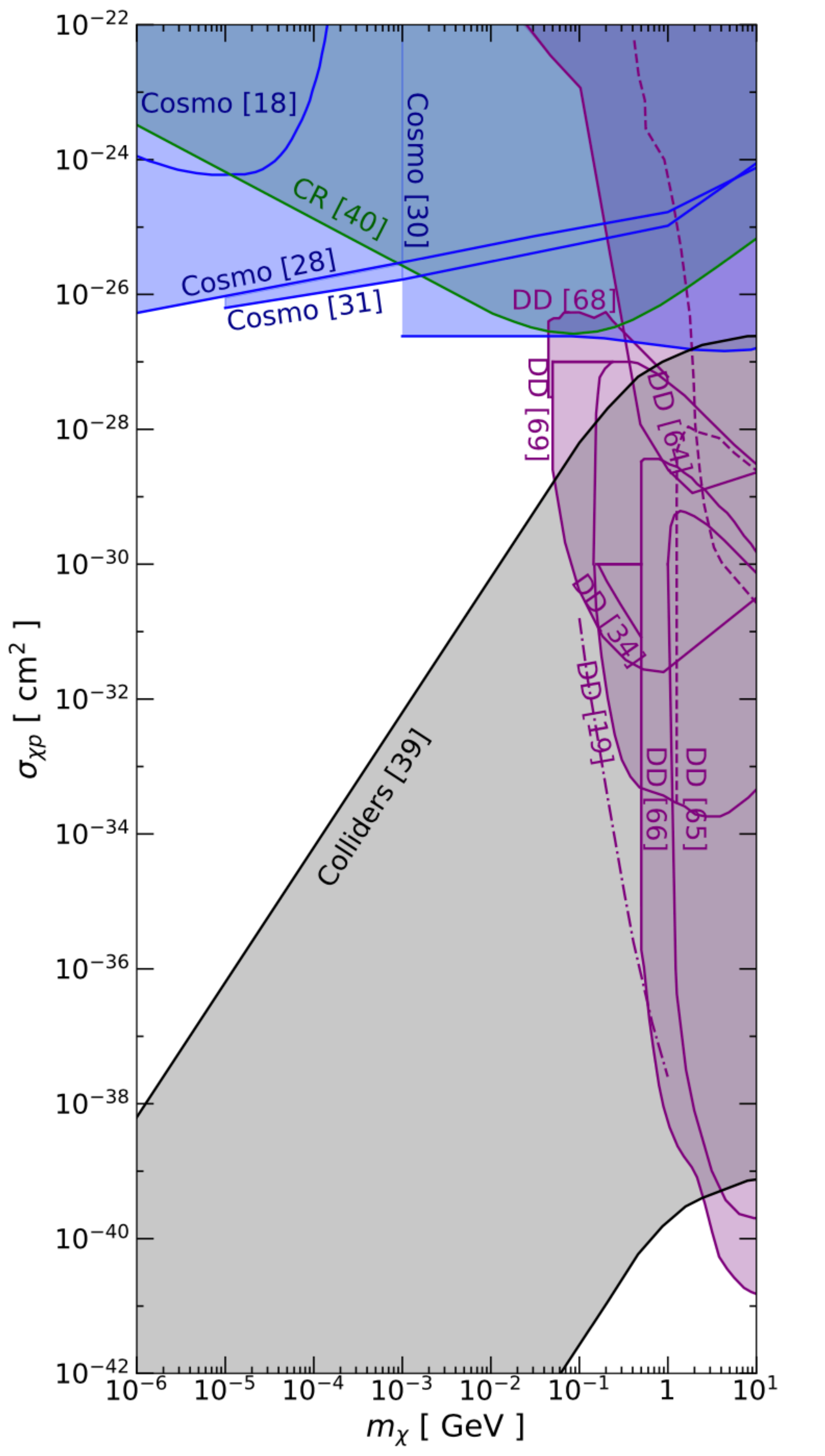

DM interactions with LHC detectors

[Bai & Rajaraman 1109.6009]

[Daci et al., 1503.05505]

[Bauer et al., 2005.13551]

[Emken+ 1905.06348]

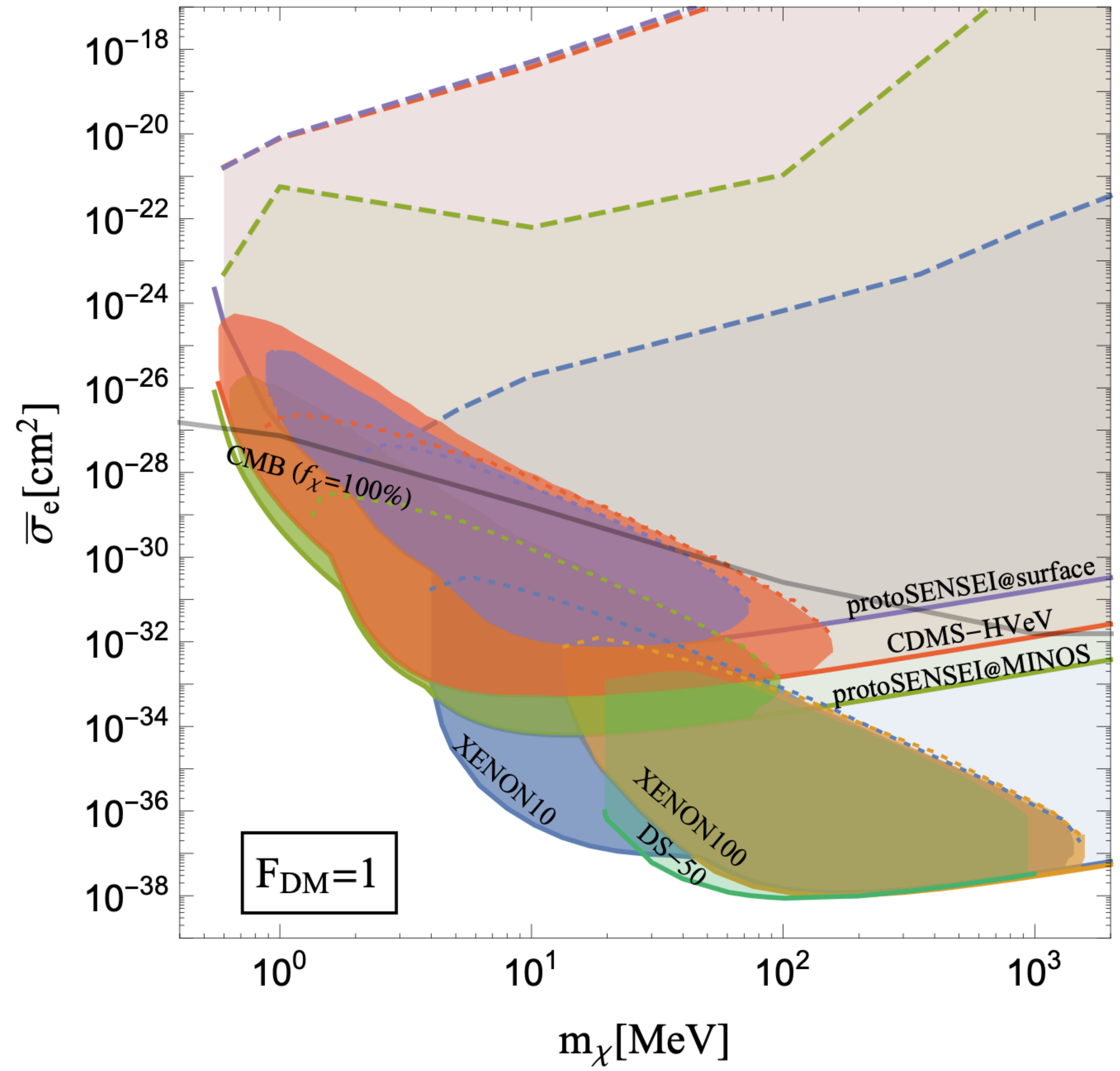

DM scattering w/ ECL @ Belle II

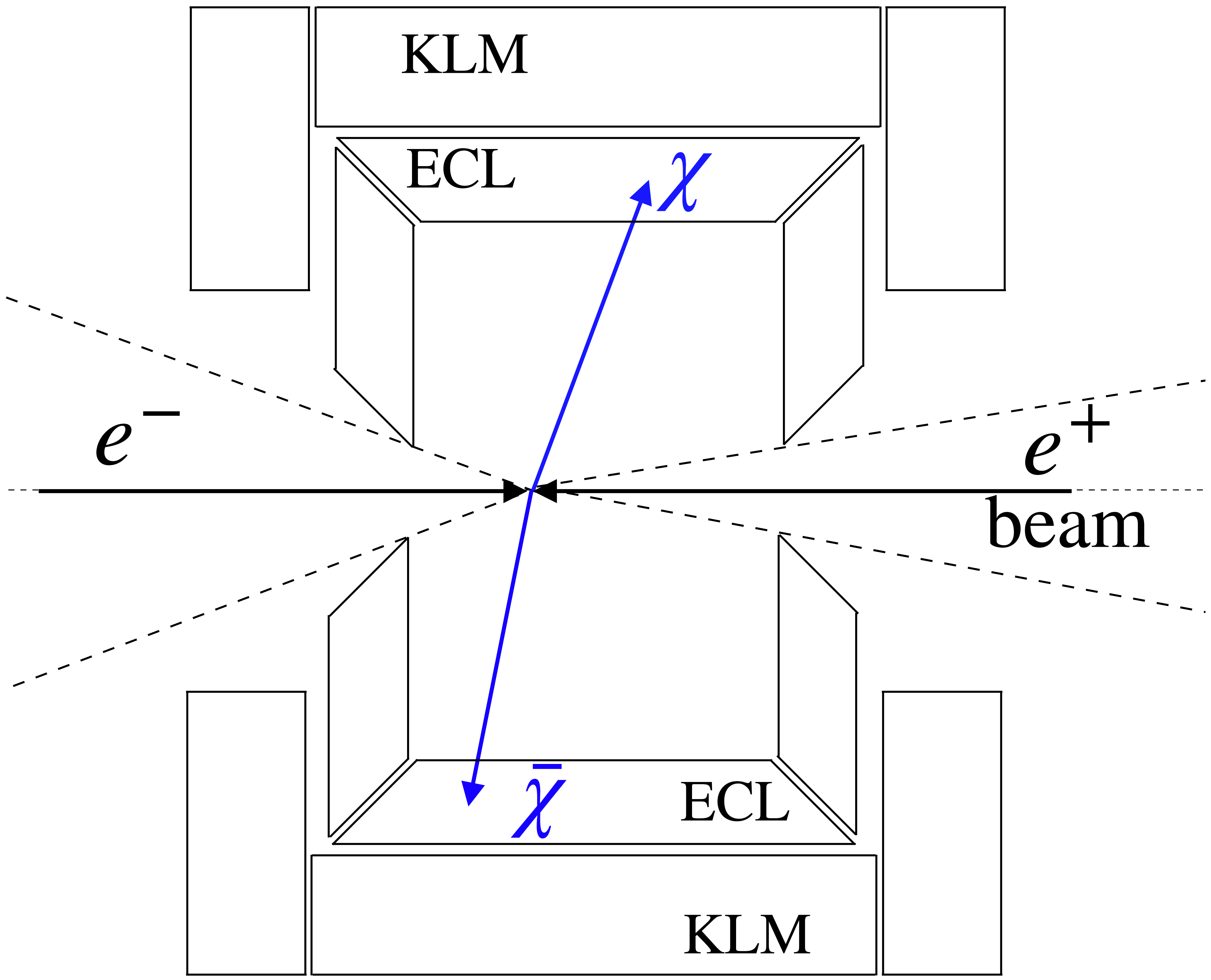

DM interacts strongly w detector

⇒multiple electron recoils

⇒ "cluster"

similar to SM photon

DM: $E_{\rm cluster} \leq E_\chi - m_\chi$

mono-cluster & di-cluster to DM

Strong DM-electron interaction via a light mediator

spin-1 (vector)	$\mathscr{L}^V_{\rm int} = Z'_\mu(g^V_\chi \bar{\chi}\gamma^\mu\chi + g^V_e \bar{e}\gamma^\mu e)$
spin-1 (axial-vector)	$\mathscr{L}^A_{\rm int} = Z'_\mu(g^A_\chi \bar{\chi}\gamma^5\gamma^\mu\chi + g^A_e \bar{e}\gamma^5\gamma^\mu e)$
spin-0 (scalar)	$\mathscr{L}^S_{\rm int} = \phi(g^S_\chi \bar{\chi}\chi + g^S_e \bar{e}e)$
spin-0 (pseudo-scalar)	$\mathscr{L}^P_{\rm int} = \phi(ig^P_\chi \bar{\chi}\gamma^5\chi + ig^P_e \bar{e}\gamma^5 e)$

a light mediator is needed for a large xsec

Belle II sensitivity versus DMDD (10 MeV mediator)

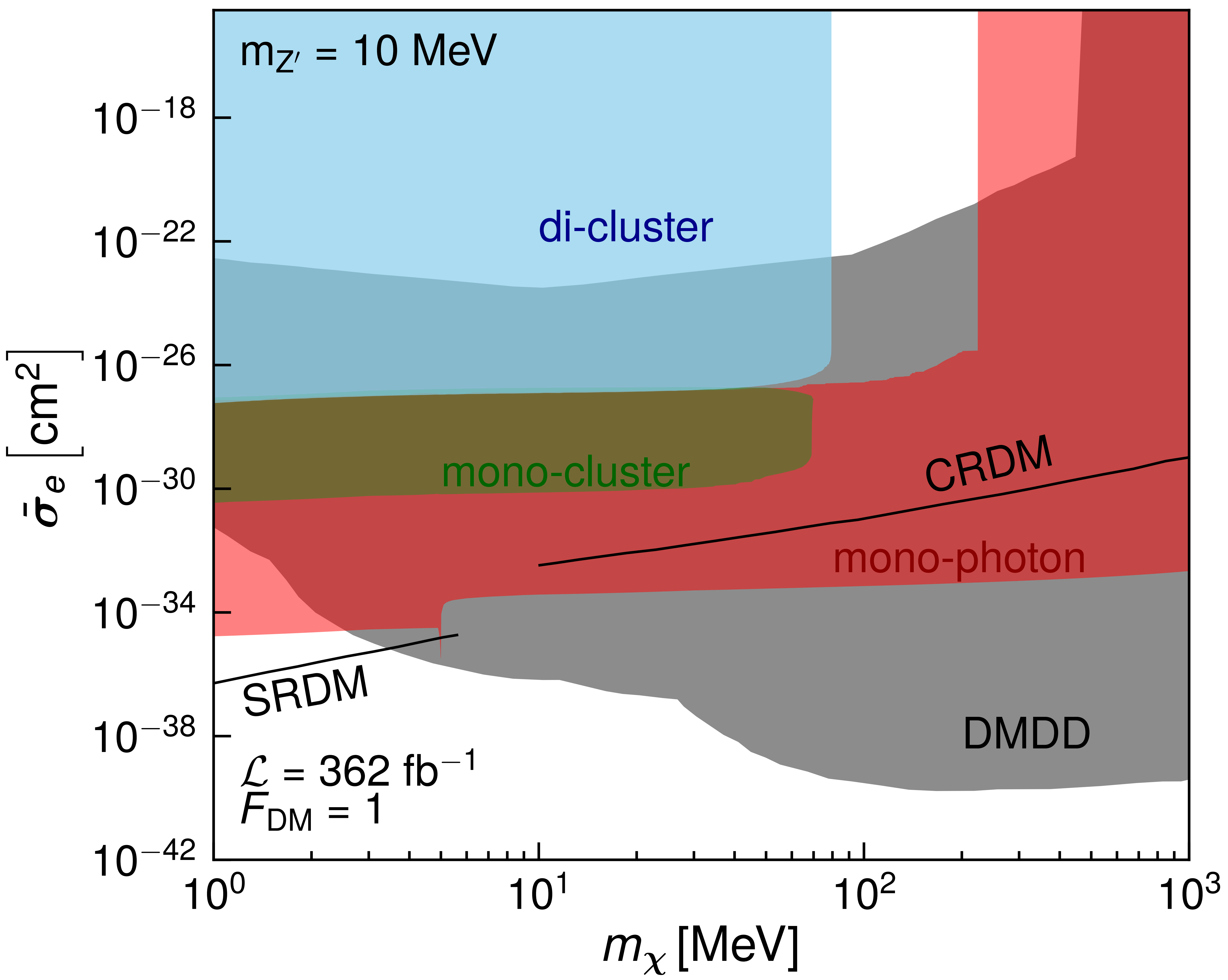

DMDD xsec @ $|q| = \alpha m_e$

FF = 1

- mono-photon
- mono-cluster
- di-cluster

large xsec excluded by colliders

[Liang, ZL, Yang, 2312.08970]

Experimental constrains on mediators

electron g-2 & NA64

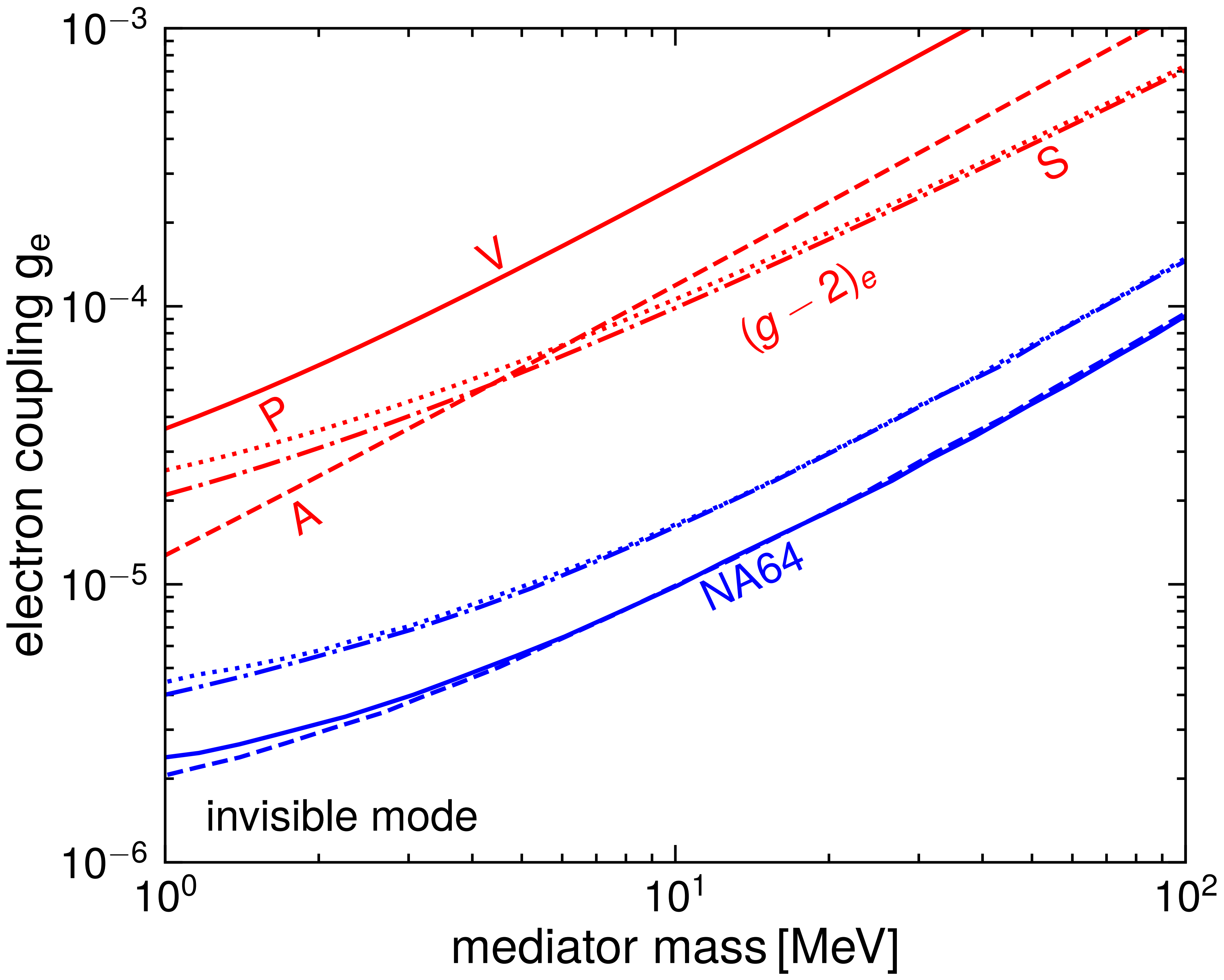

invisible scenario

electron beam-dump & collider

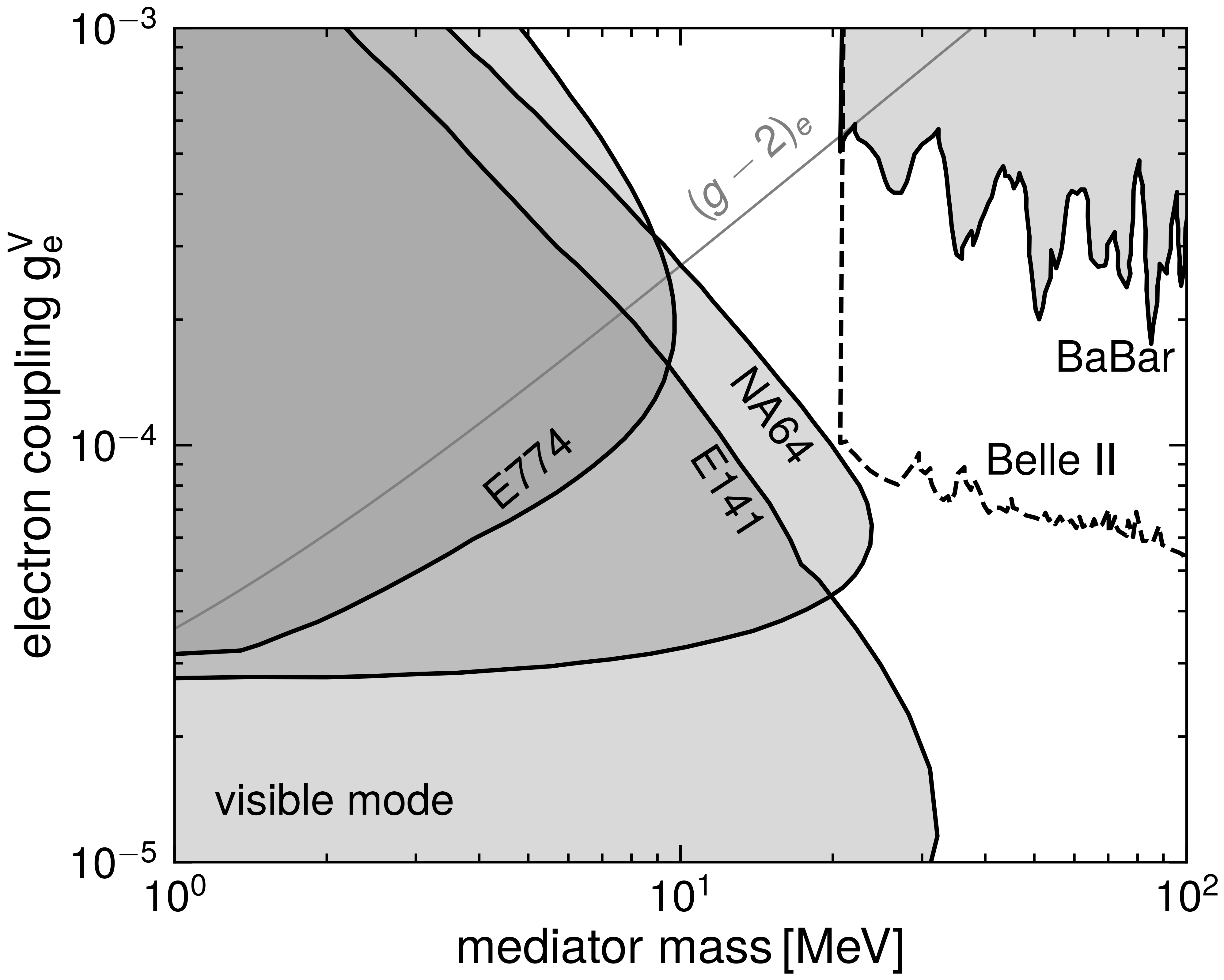

visible scenario

Belle II sensitivity versus DMDD (ultralight mediator)

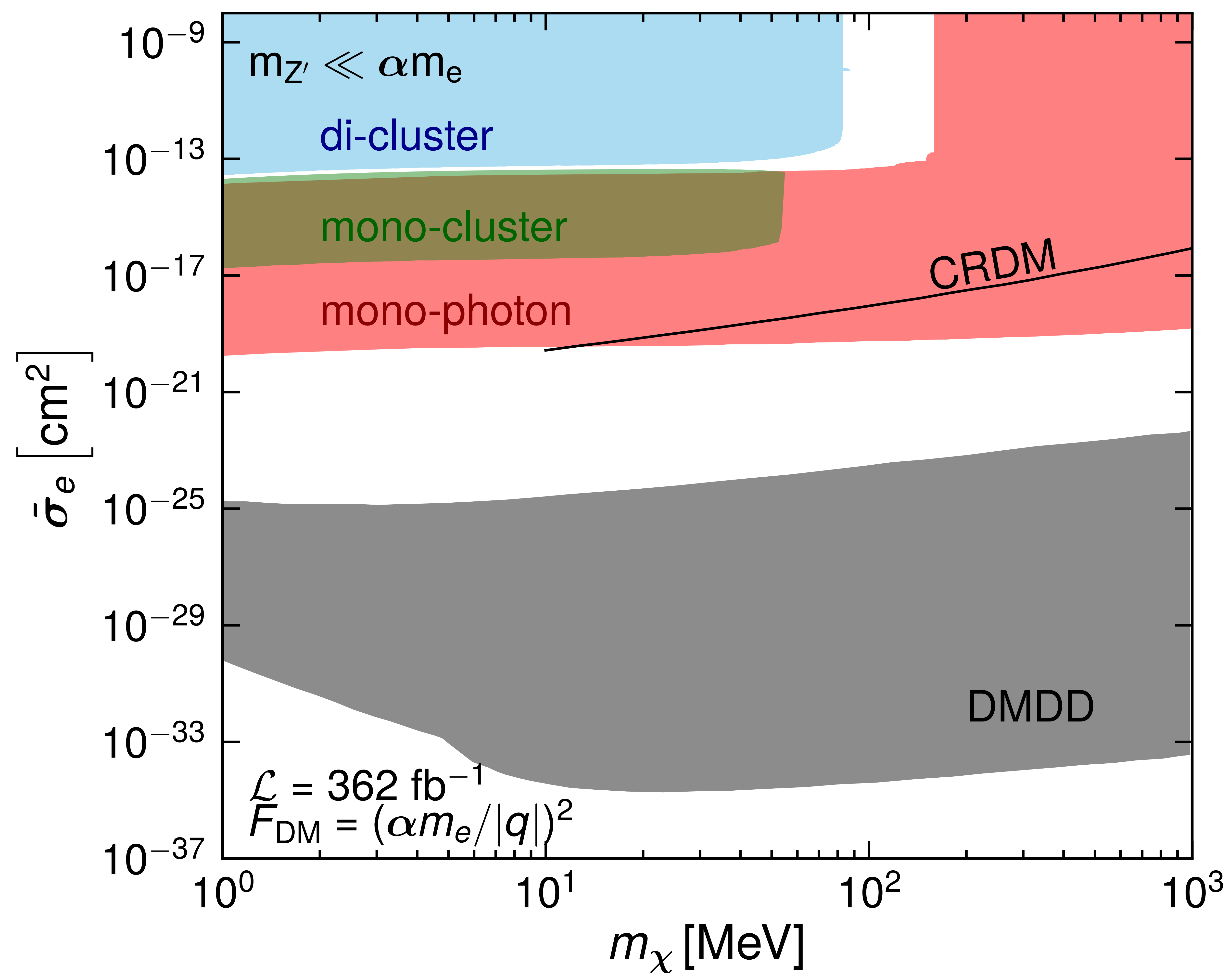

FF $\propto |q|^{-2}$

large xsec excluded by colliders

allowed para space between colliders & DMDD

[Liang, ZL, Yang, 2312.08970]

Summary

- New dark matter channel at electron colliders **[Liang, ZL, Yang, 2212.04252]**
  - Fixed target inside electron collider: positron collisions with detector
  - Probe new parameter space of invisible dark photon, surpassing both the mono-photon channel at Belle II & the missing momentum search at NA64.
- Electron collider constraints on strongly-interacting dark matter
  - DM-induced mono-cluster or di-cluster signatures **[Liang, ZL, Yang, 2312.08970]**
  - Current Belle II data can probe the parameter space w/ a large cross section, which is often difficult to probe in DMDD & DMID experiments.

backup slides

Kinetic mixing & mass mixing

$SU(3)_c \times SU(2)_L \times U(1)_Y \times U(1)_X$

[Feldman, ZL, Nath, hep-ph/0702123, 391 cites]

$$\mathscr{L} = -\frac{1}{4}B_{\mu\nu}B^{\mu\nu} - \frac{1}{4}X_{\mu\nu}X^{\mu\nu} + g_D X_\mu \bar{\chi}\gamma^\mu \chi - \frac{\tilde{\delta}}{2} B_{\mu\nu} X^{\mu\nu} - \frac{M_1^2}{2}(\partial_\mu \sigma + X_\mu + \tilde{\epsilon} B_\mu)^2$$

kinetic mixing

mass mixing

kinetic mixing $\tilde{\delta}$ & mass mixing $\tilde{\epsilon}$ are degenerate (w/o χ): only $\epsilon \sim (\tilde{\epsilon} - \tilde{\delta})$ is physical

Comparison with primordial black hole

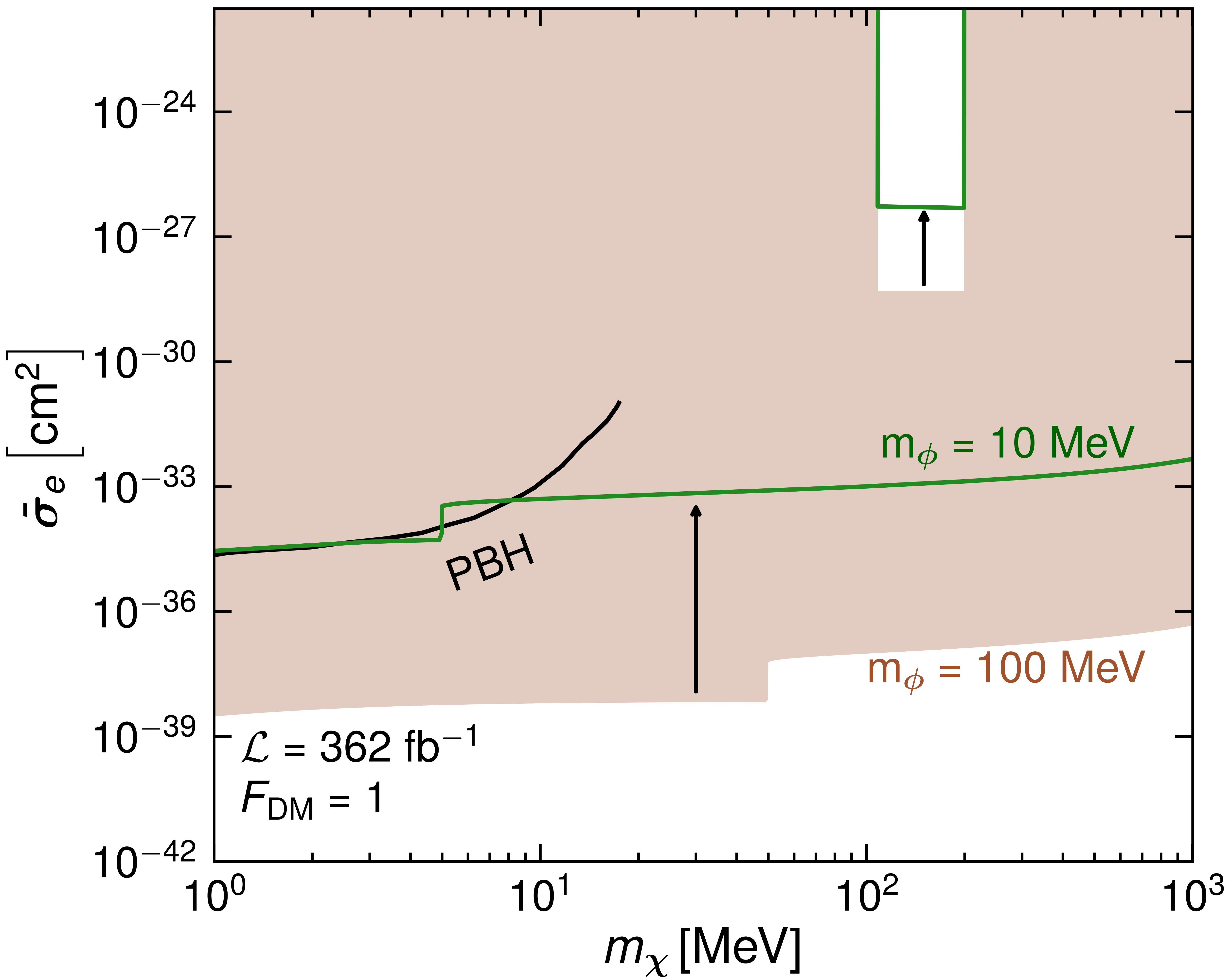

BSM particle w/ mass below Hawking temperature can be produced in PBH ⇒ ER @ SK

PBH $E = 10$ MeV

detection via $\bar{\chi}\chi\bar{e}e/\Lambda^2$

[Calabrese+, 2203.17093]

Comparison with primordial black hole

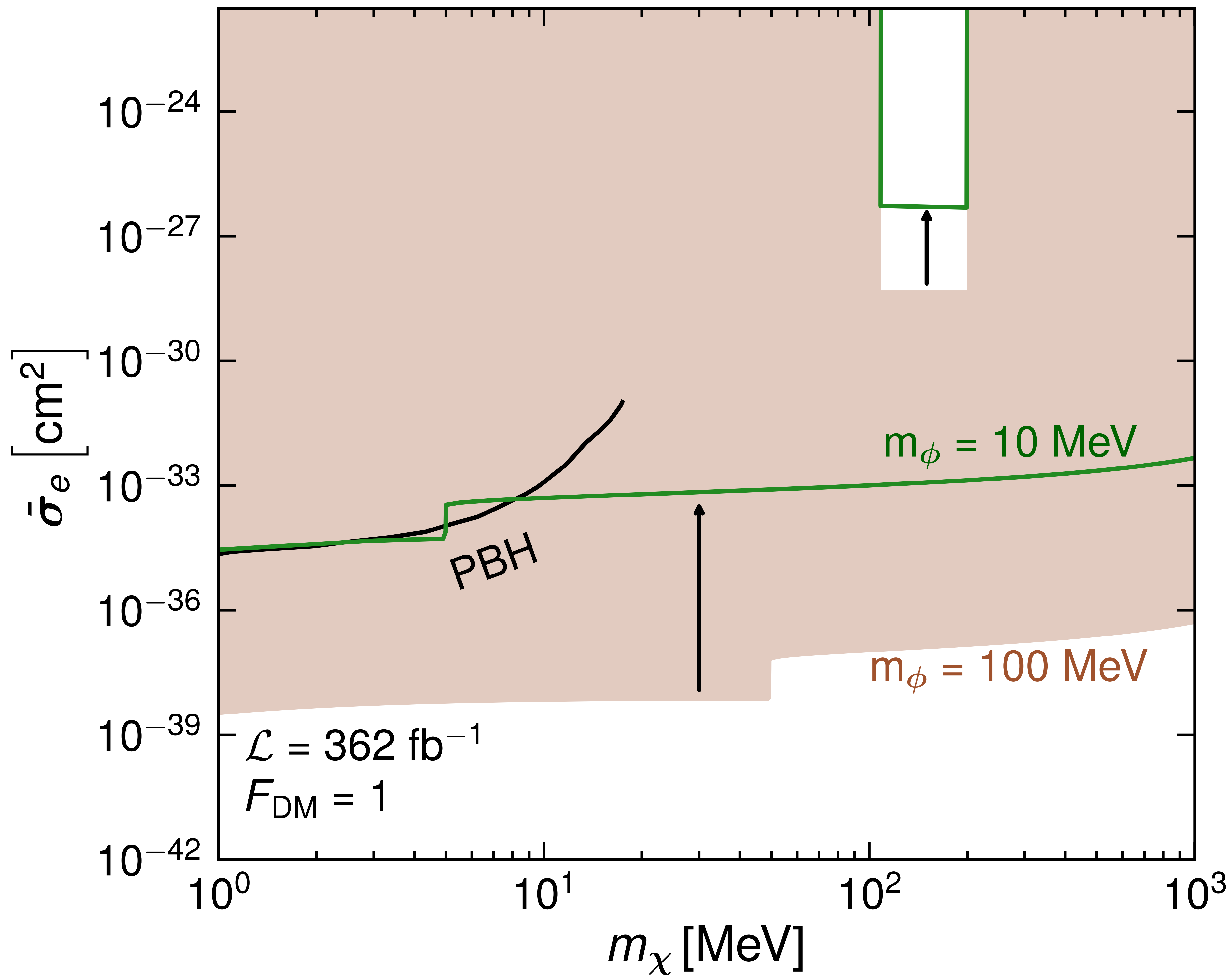

BSM particle w/ mass below Hawking temperature can be produced in PBH ⇒ ER @ SK

PBH $E = 10$ MeV

detection via $\bar{\chi}\chi\bar{e}e/\Lambda^2$

[Calabrese+, 2203.17093]

Belle II limits for the scalar mediator

- 10^4 times better w/ m = 100 MeV
- similar to PBH w/ m = 10 MeV

CRBG for DP m < 2 GeV

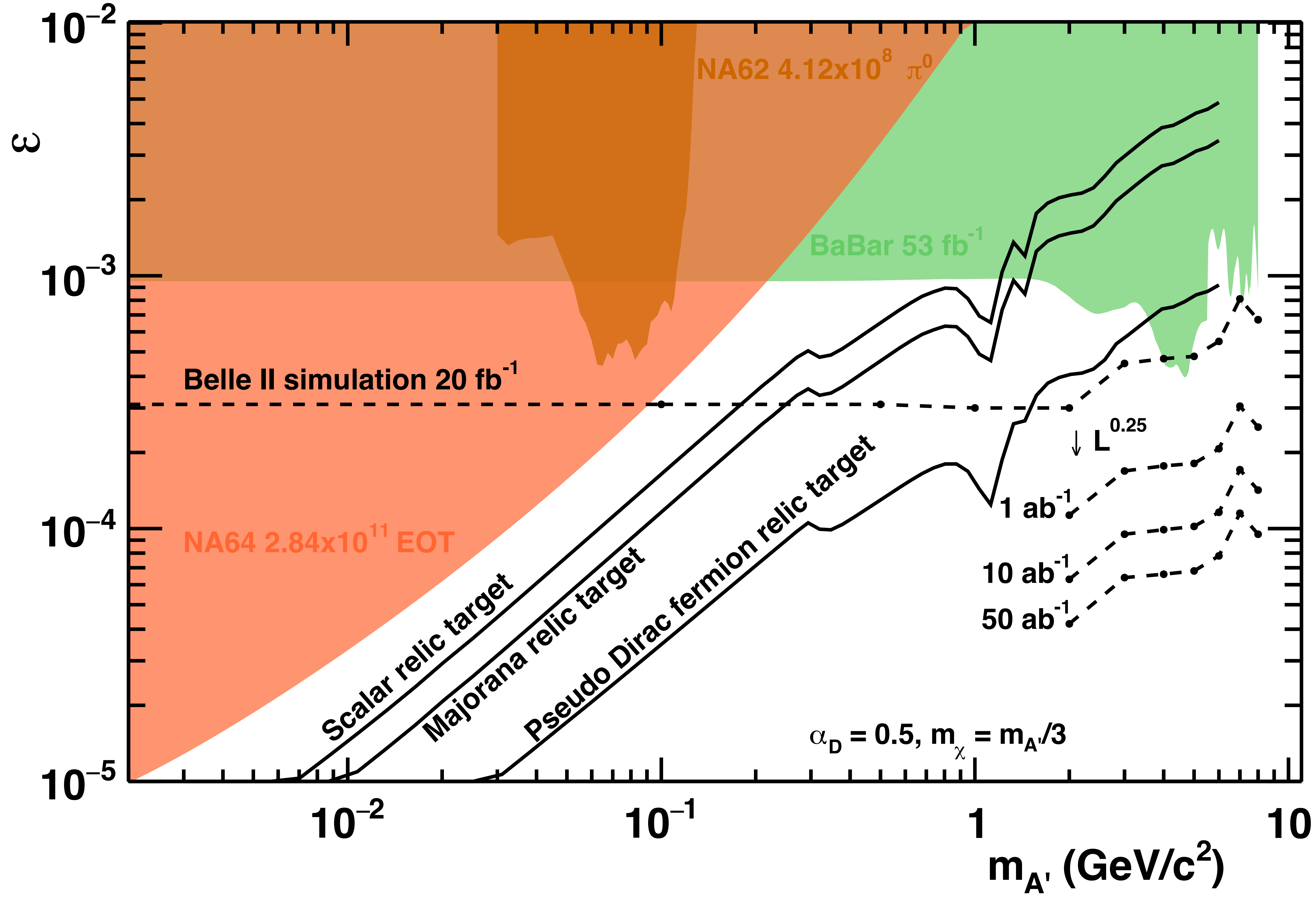

potential CRBG for DP m < 2 GeV [2207.06307]

Scalar mediator

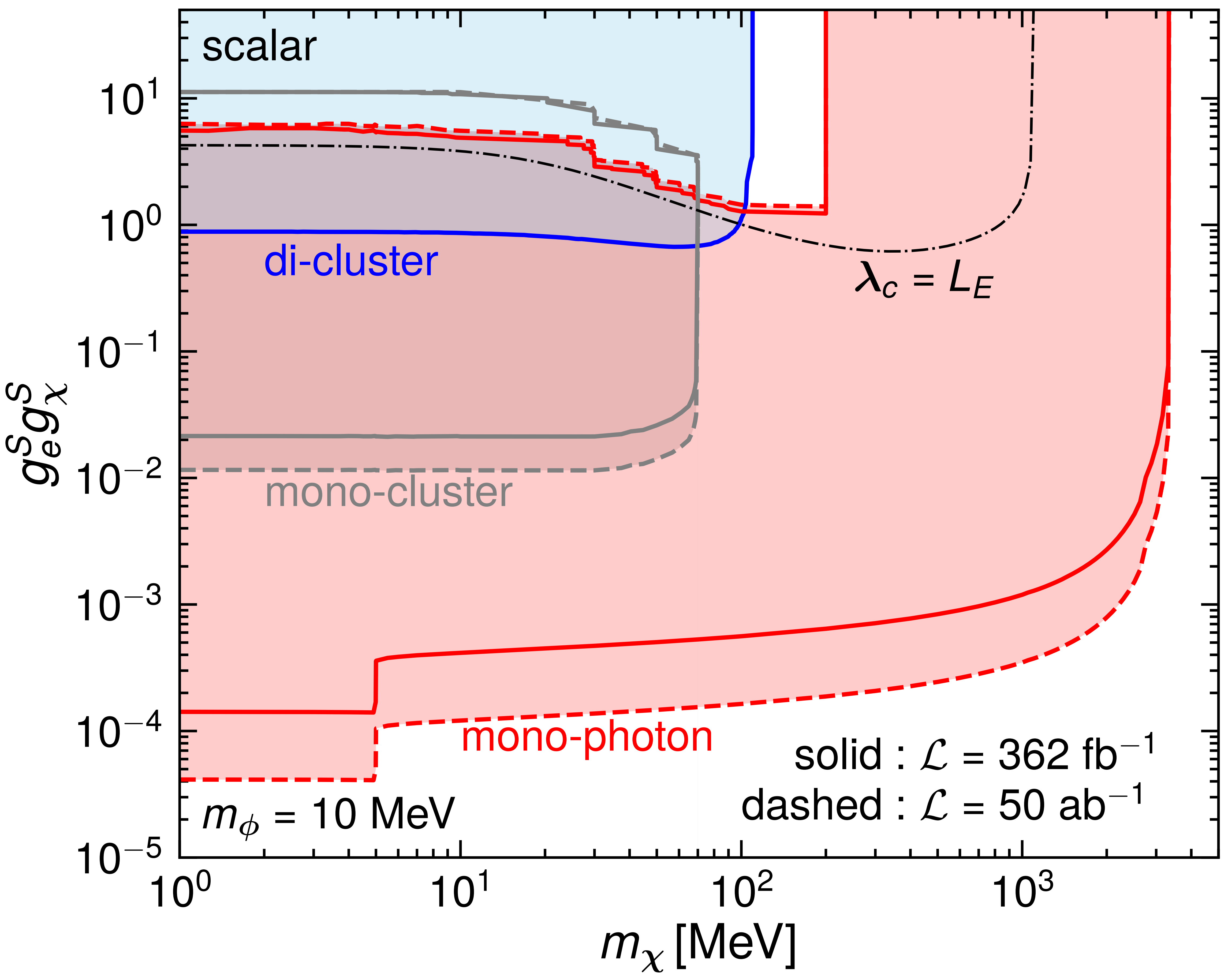

mediator mass = 10 MeV

ceiling of mono-photon

di-cluster probes large couplings

Pseudo-scalar mediator

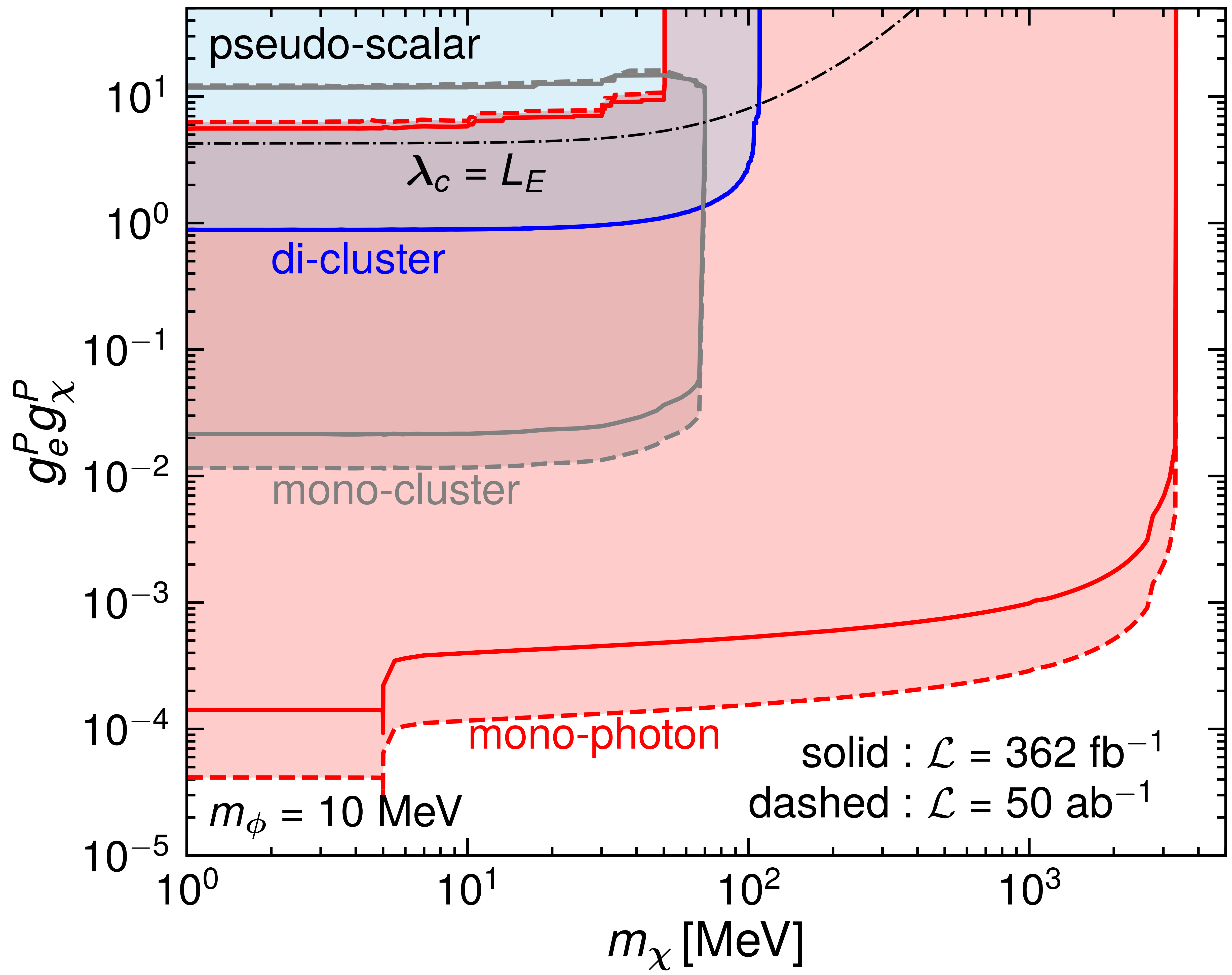

mediator mass = 10 MeV

Vector & axial-vector couplings

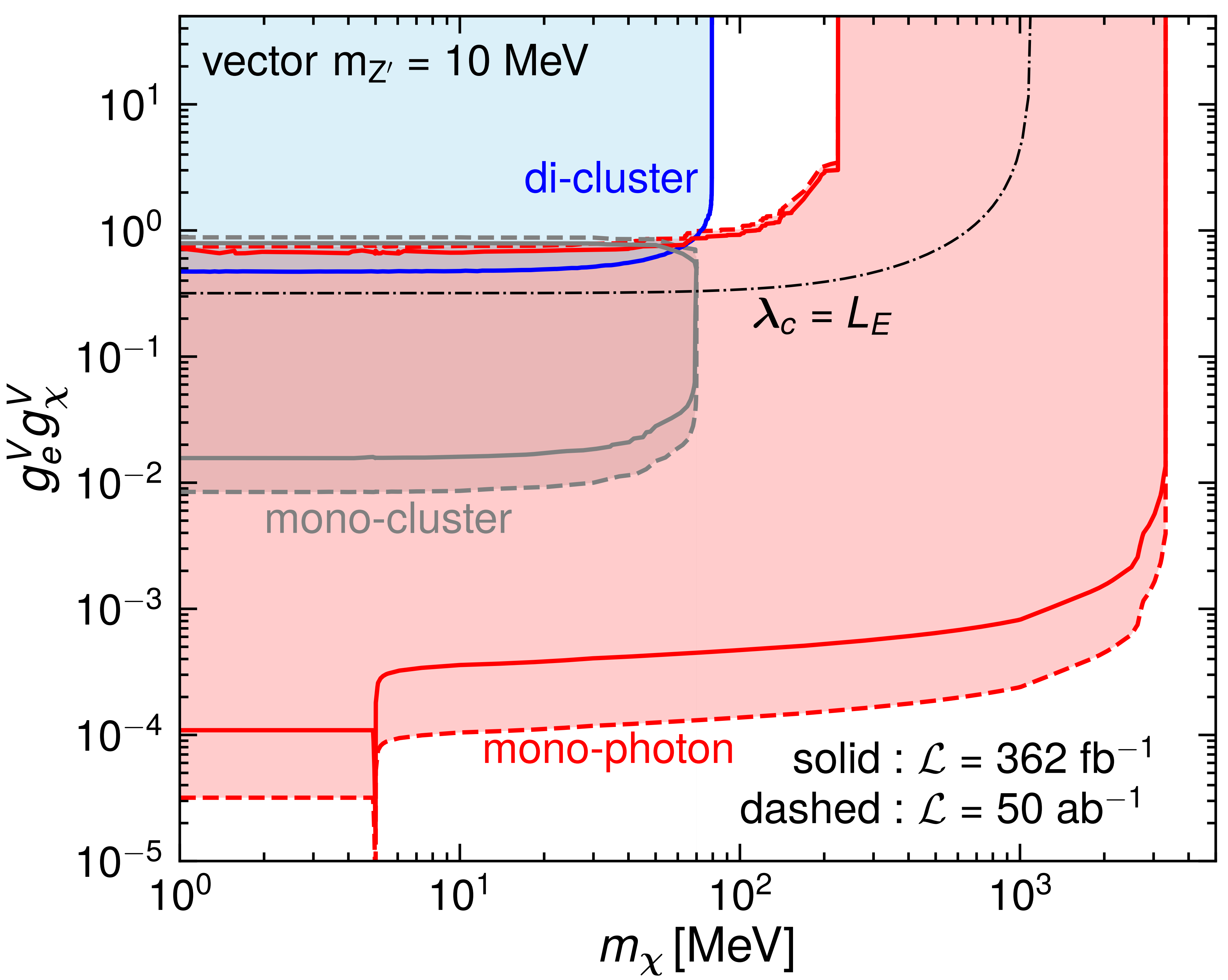

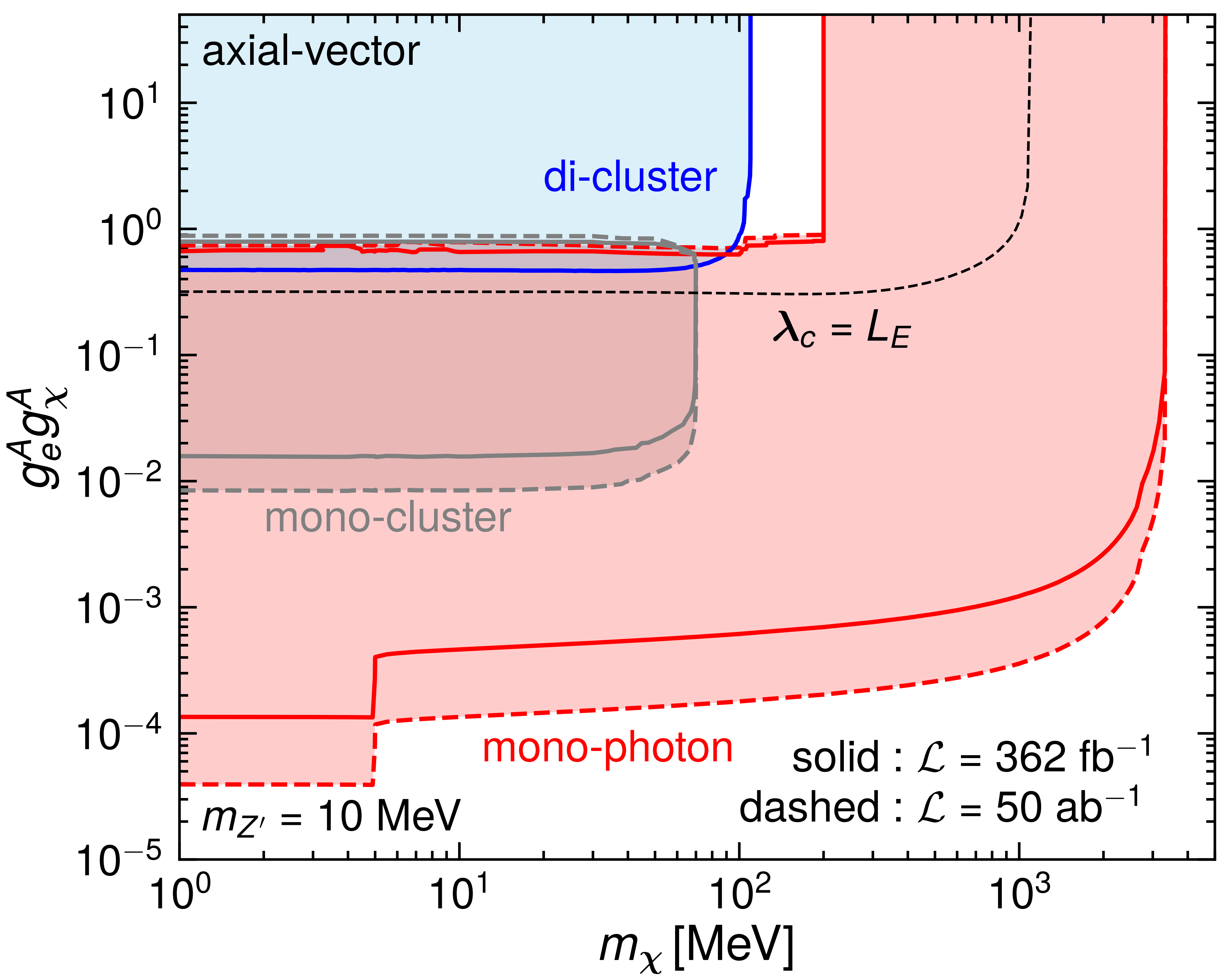

mediator mass = 10 MeV

[Liang, ZL, Yang, 2312.08970]

Scalar & pseudo-scalar

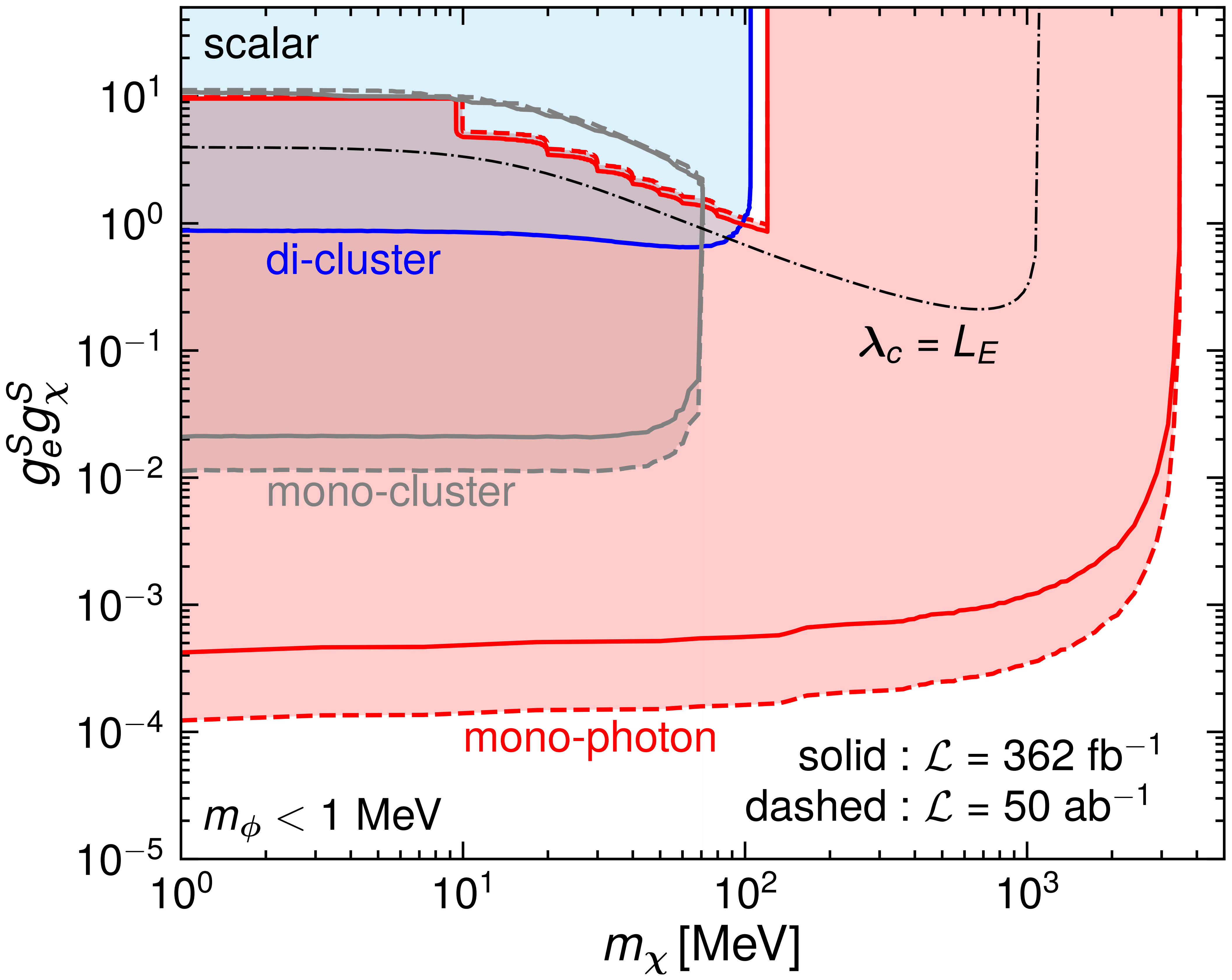

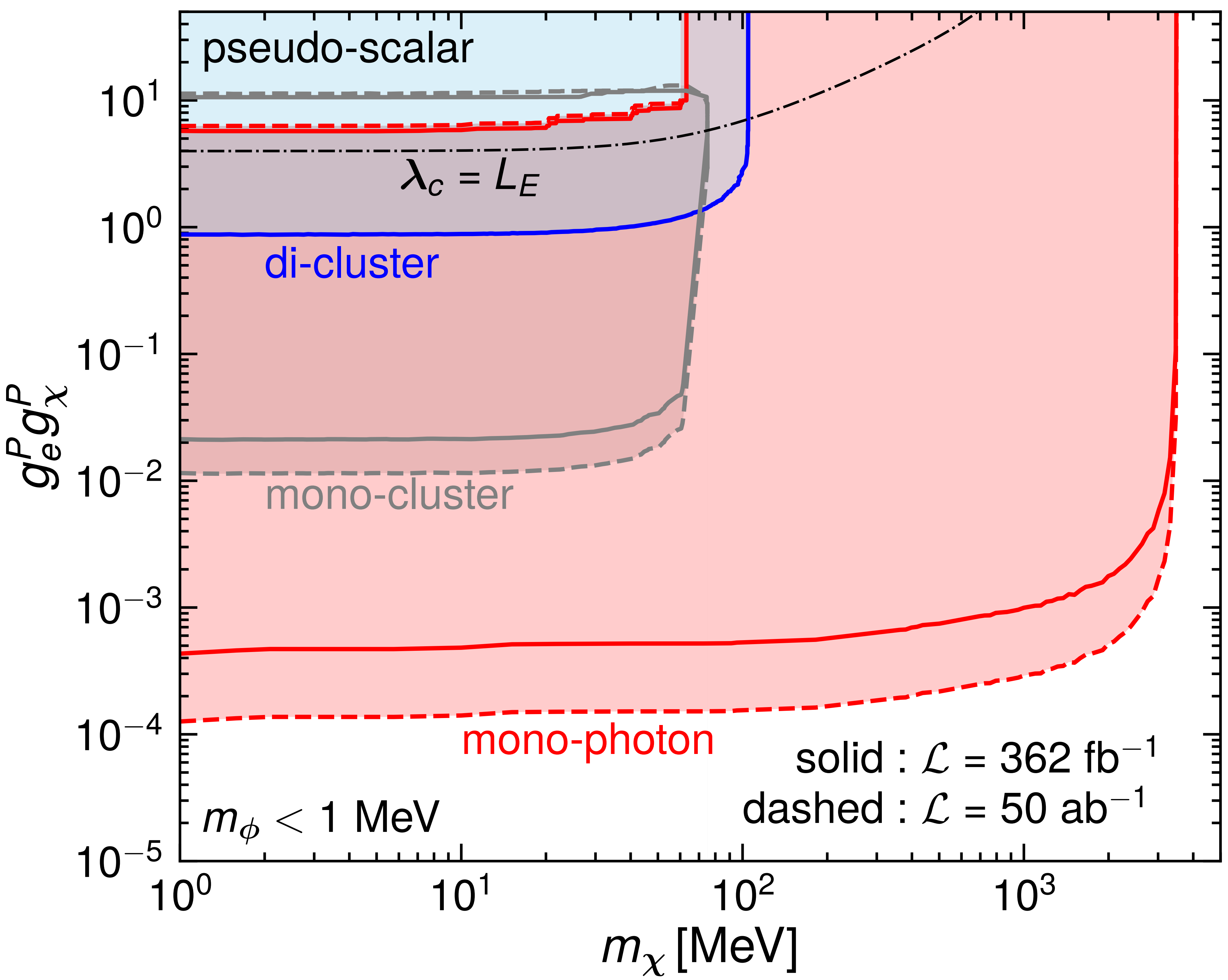

mediator mass = 1 MeV

Vector & axial-vector

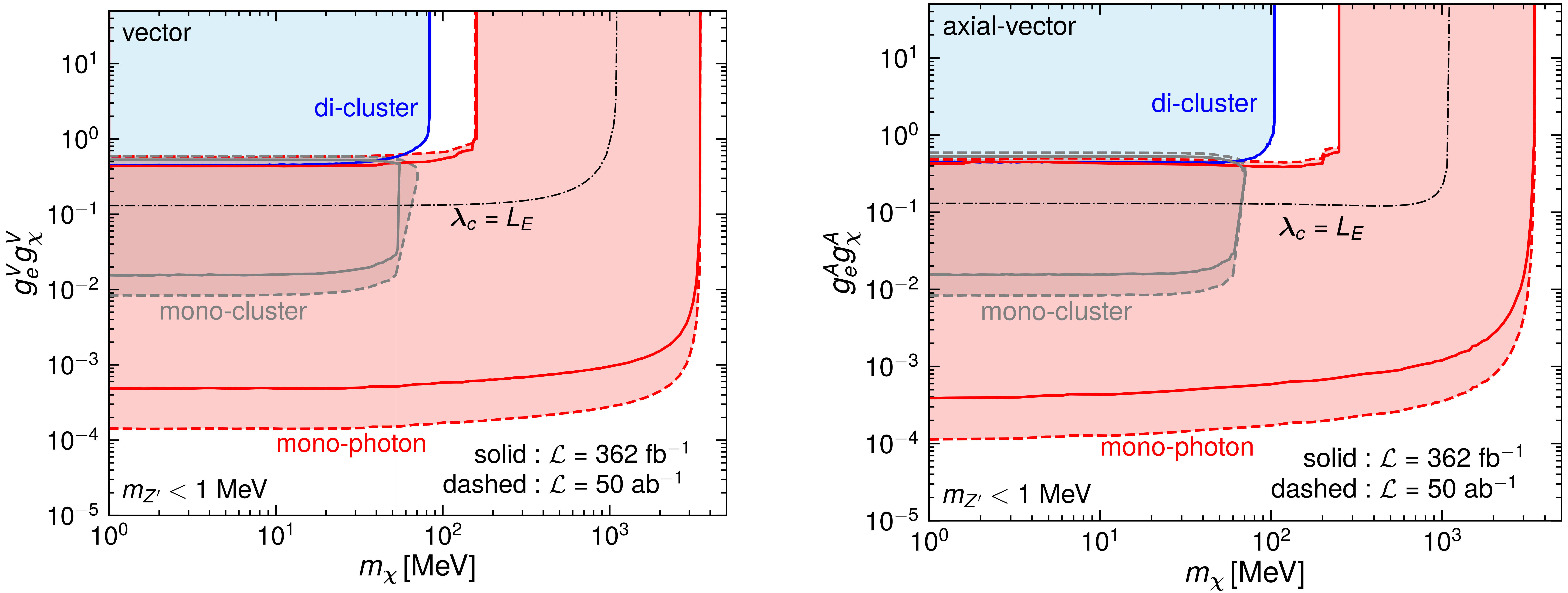

mediator mass = 1 MeV

electron g-2

as shown in Fig. (3). The contributions to the electron $g-2$ from the mediators in Eqs. (14-17) are [64–66]

$$\Delta a_e^{\rm NP} = \frac{g_e^2\lambda^2}{8\pi^2}\int_0^1 dx \frac{Q(x)}{(1-x)(1-\lambda^2 x)+\lambda^2 x}, \quad (18)$$

where $\lambda = m_e/m$ with m_e (m) being the electron (mediator) mass, g_e denotes the various couplings to electrons in Eqs. (14-17), and $Q(x)$ are

$$Q_V = 2x^2(1-x), \quad (19)$$
$$Q_A = 2x(1-x)(x-4) - 4\lambda^2 x^3, \quad (20)$$
$$Q_S = x^2(2-x), \quad (21)$$
$$Q_P = -x^3, \quad (22)$$

where the subscript denotes the four types of mediators in Eqs. (14-17).

The interpretation of electron $g-2$ data depends on the experimental determination of the fine structure constant α. By using the α value measured with rubidium (Rb) atoms [67] and cesium (Cs) atoms [68], it is shown in Ref. [69] that the new electron $g-2$ measurement [70] has a 2.2 σ and -3.7 σ deviations from the SM prediction [71]:

$$\Delta a_e(\text{Rb}) = (34 \pm 16) \times 10^{-14}, \quad (23)$$
$$\Delta a_e(\text{Cs}) = (-101 \pm 27) \times 10^{-14}. \quad (24)$$

Given the intricate aspects of this measurement, we adopt a cautious approach in constraining new physics models: We add a 2σ to the central deviations in Eqs. (23-24) and then use the largest deviation to constrain new physics contributions regardless the sign. Thus, the new physics contributions should satisfy

$$|\Delta a_e^{\rm NP}| \lesssim 155 \times 10^{-14}. \quad (25)$$

Fig. (4) shows the constraints on the four types of mediators in Eqs. (14-17).

Track length

For positrons with initial energy E to enter a target with thickness L_T, the differential track-length distribution as a function of the positron energy E' can be computed by [1, 2]

$$T_e(E', E, L_T) = X_0 \int_0^{L_T/X_0} I_e(E', E, t) dt, \tag{1}$$

where X_0 is the radiation length of the target. Here $I_e(E', E, t)$ is the energy distribution of E' at the depth tX_0, which can be computed iteratively such that $I_e = \sum_i I_e^{(i)}$ where $I_e^{(i)}$ denotes the i-th generation positrons [3]. We adopt the analytical model of Ref. [3] up to second-generation positrons, which are found to be in good agreement with simulations in Ref. [1]. The contributions from the first two generations are [3]

$$I_e^{(1)}(E', E, t) = \frac{1}{E} \frac{(\ln(1/v))^{b_1 t - 1}}{\Gamma(b_1 t)}, \tag{2}$$

$$I_e^{(2)}(E', E, t) = \frac{2}{E} \int_v^1 \frac{dx}{x^2} \frac{1}{b_2 + b_1 \ln(1-x)} \left[\frac{(1-x)^{b_1 t} - (1-v/x)^{b_1 t}}{b_1 \ln\left[(x-x^2)/(x-v)\right]} + \frac{e^{-b_2 t} - (1-v/x)^{b_1 t}}{b_2 + b_1 \ln(1-v/x)} \right], \tag{3}$$

where $b_1 = 4/3$, $b_2 = 7/9$, $v = E'/E$.

[1] 1802.03794
[2] 1807.05884
[3] Tsai & Whitis 1966

xsec of on-shell dark photon

where n_N is the number density of I (or Cs). Here $d\sigma_{\rm bre}/dE_{A'}$ is the differential cross section of the on-shell produced A' [71–73],

$$\frac{d\sigma_{\rm bre}}{dE_{A'}} = (\phi_I + \phi_{\rm Cs})\frac{4\alpha^3\epsilon^2}{E'}\frac{x(1-x+x^2/3)}{m_{A'}^2(1-x)+m_e^2x^2}, \qquad (13)$$

where $x \equiv E_{A'}/E'$, and ϕ_N denotes the effective flux of photons from nucleus N [71]:

$$\phi_N = \int_{t_{\rm min}}^{t_{\rm max}} dt\,\frac{t-t_{\rm min}}{t^2}\left[\frac{Za^2t}{(1+a^2t)(1+t/d)}\right]^2, \qquad (14)$$

with $t_{\rm min} = (m_{A'}^2/2E')^2$, $t_{\rm max} = m_{A'}^2 + m_e^2$, $a = 111m_e^{-1}Z^{-1/3}$, and $d = 0.164A^{-2/3}$ GeV^2. We use $Z = 53\,(55)$ and $A = 127\,(133)$ for I (Cs). Here we only consider the dominant elastic form factor.

[71] Bjorken et al, 0906.0580
[72] Gninenko et al, 171205706
[73] Liu & Miller, 1705.01633

Selection in GEANT4 simulations

At least 1 neutron with energy > 3 GeV

Energy deposition in ECL < 5%

Veto $p/\pi^{\pm}$ with momentum > 0.6 GeV (either deposit energy in ECL or produce tracks in KLM)

Count # of neutrons with K.E. > 280 MeV (hadronic shower threshold)

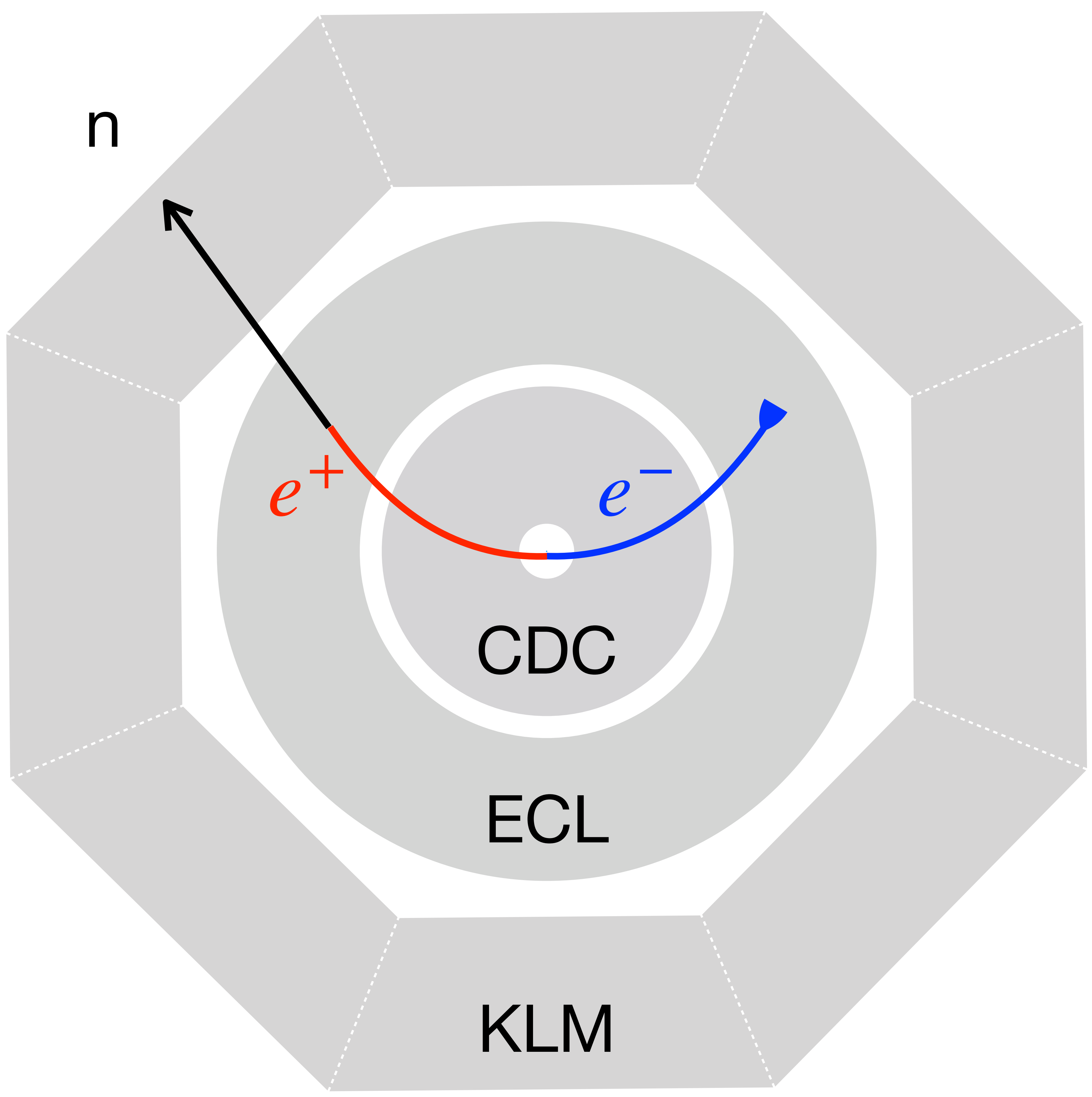

Experimental constraints on light mediators

- Electron g-2

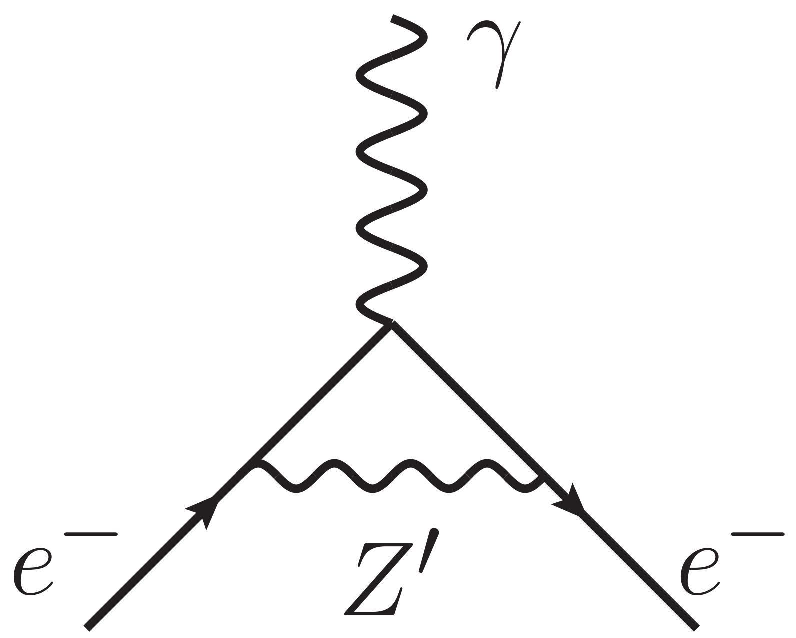

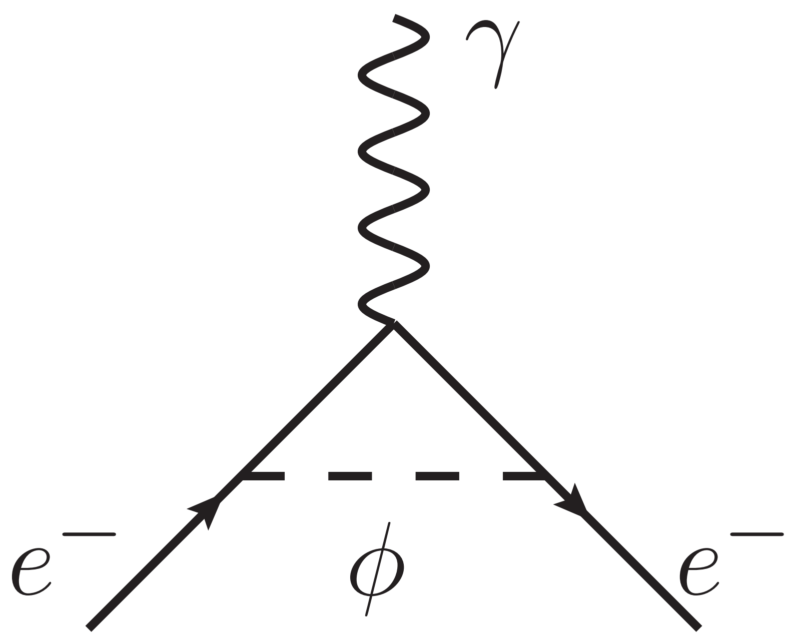

- Electron beam dump & BaBar
  - visible mode
  - invisible mode

- Moller scattering (SLAC E158) $|g_e^V g_e^A| \lesssim 10^{-8}$